CHAPTER 5

Geochemistry

5.1 Element Mobility

Although the studied mafic to felsic volcanic/hypabyssal rocks were carefully selected, their chemical compositions are unlikely to represent those in magma since the rocks have undergone variable degrees of alteration and low-grade metamorphism (see Chapter 4). The concentrations of immobile elements may be changed, due to the dilution or enrichment of the mobile elements, however, the ratios of immobile elements in the primary rock and altered rock remain constant. Accordingly, only the elements considered as immobile elements and immobile-element ratios are used to interpret the geochemical data in this study.

Almost all the major oxides, excluding some certain minor oxides, in ancient igneous rocks are sensitive to alteration/metamorphic processes (veining and distribution of calcite, quartz, albite, sericite and epidote minerals). It is, however, generally agreed that the values of total iron and MgO in the carefully selected samples of altered/metamorphosed igneous suites are little removed from primary values (Panjasawatwong *et al.,* 2006). According to the little mobility of total iron and MgO, and their significant abundances in mafic volcanic rocks, total iron as FeO (herein FeO*)/ MgO ratios are used as a fractionation parameter for the studied least-altered mafic to felsic volcanic/hypabyssal rock samples.

Following the work pioneered by Pearce and Cann (1971, 1973), numerous studies have shown that the high field strength elements (herein HFSE) Ti, Zr, Y, Nb, Ta, Th, U, P and also the transitional elements Ni, Cr, V and Sc are relatively immobile during the alteration of basaltic and more evolved lavas and intrusives (e.g. Floyd and Winchester, 1975; Pearce and Gale, 1977; Winchester and Floyd, 1977; Pearce and Norry, 1979; Pearce, 1982; Shervais, 1982; Meschede, 1986). In addition, although occasional reports have appeared of REE-, especially light REE (herein LREE), mobility during

hydrothermal alteration and low-grade metamorphism (e.g. Hellman and Henderson, 1979; Whitford *et al*., 1988), the overwhelming consensus of opinion is that the REE patterns of carefully selected igneous samples are probably slightly shifted from their primary patterns, but remain parallel/sub-parallel to the primary patterns. Consequently, in attempting to determine the geochemical affinities and tectonic significance of the studied least-altered mafic to felsic volcanic/hypabyssal rocks, concentration has focused on the relatively immobile elements, namely high field strength elements (herein HFSE), REE and transition elements. Furthermore, Zr is an incompatible immobile element, therefore it will be used as a fractionation parameter for the studied least-altered mafic to felsic volcanic/hypabyssal rock samples.

5.2 Magmatic Affinity

The studied least-altered mafic to felsic volcanic/hypabyssal rocks are classified by Zr/TiO_2-Nb/Y diagram of Winchester and Floyd (1977) (Figure 5.1). They can be divided into five groups using REE patterns and N-MORB normalized multi-elements patterns (Figures 5.2, and 5.3) as Group I rocks (calc-alkalic), Group II rocks (calc-alkalic), Group III rocks (tholeiitic), Group IV rocks (tholeiitic) and Group V rocks (shoshonitic), and will be discussed in the next sections.

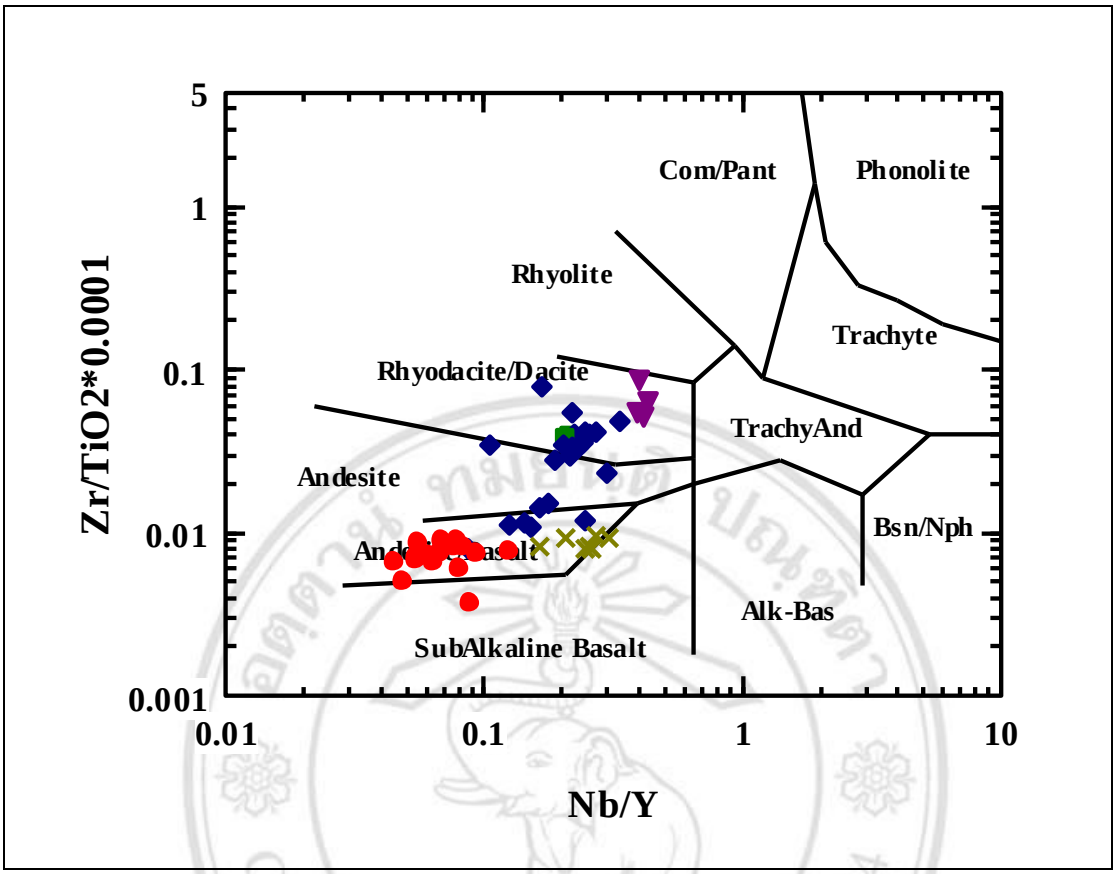

Figure 5.1 Plot of Zr/TiO_2 against Nb/Y for the studied least-altered felsic to mafic volcanic/hypabassal rocks [Group I (blue diamond), Group II (violet inverted triangle), Group III (green cross), Group IV (red circle) and Group V (green square)]. Field boundaries for different magma types are taken from Winchester and Floyd (1977).

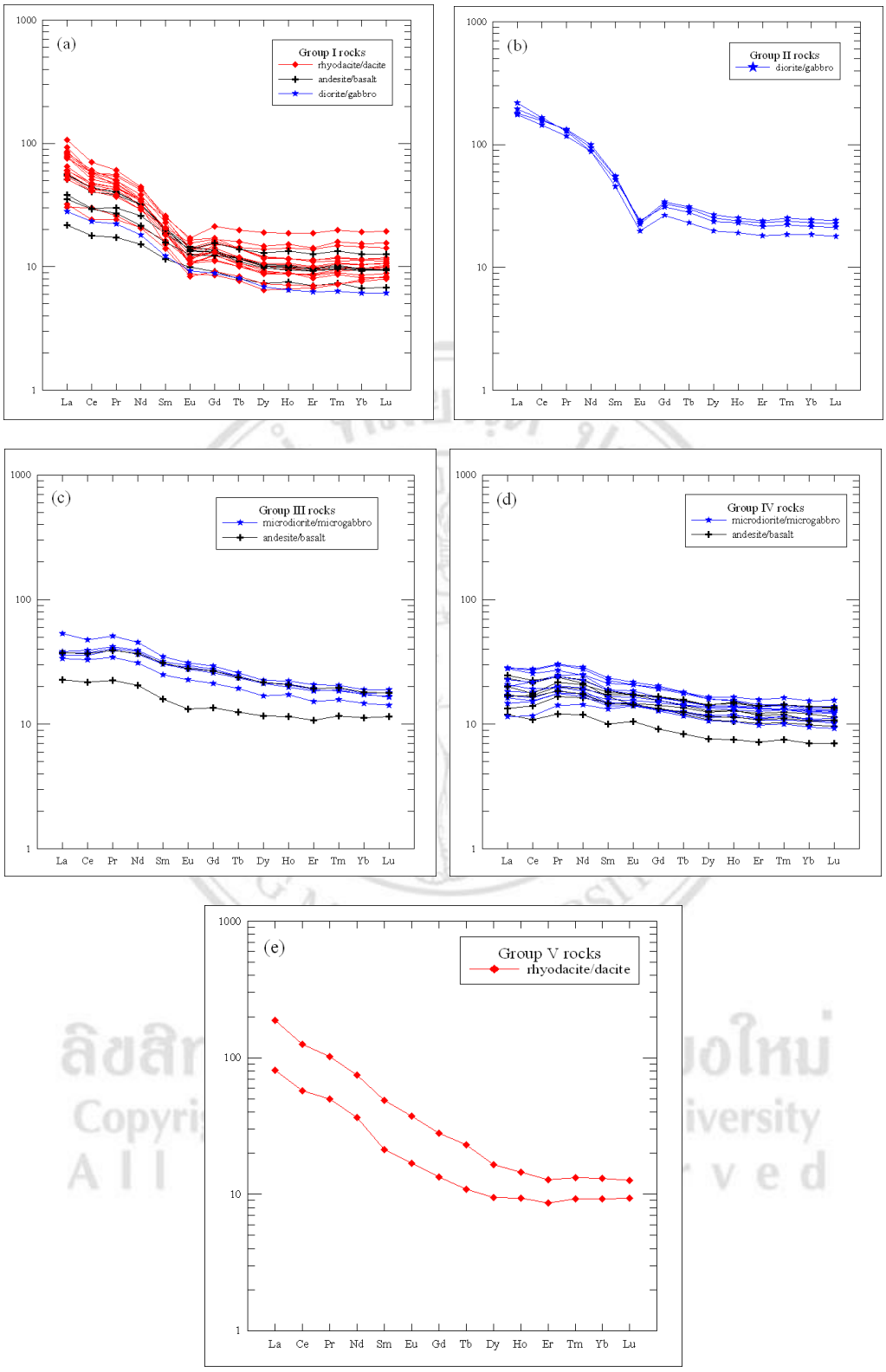

Figure 5.2 Chondrite - normalized REE patterns for the studied least-altered Group I (a), Group II (b), Group III (c), Group IV (d) and Group V (e) rocks. Normalizing values used are those of Taylor and Gorton (1977).

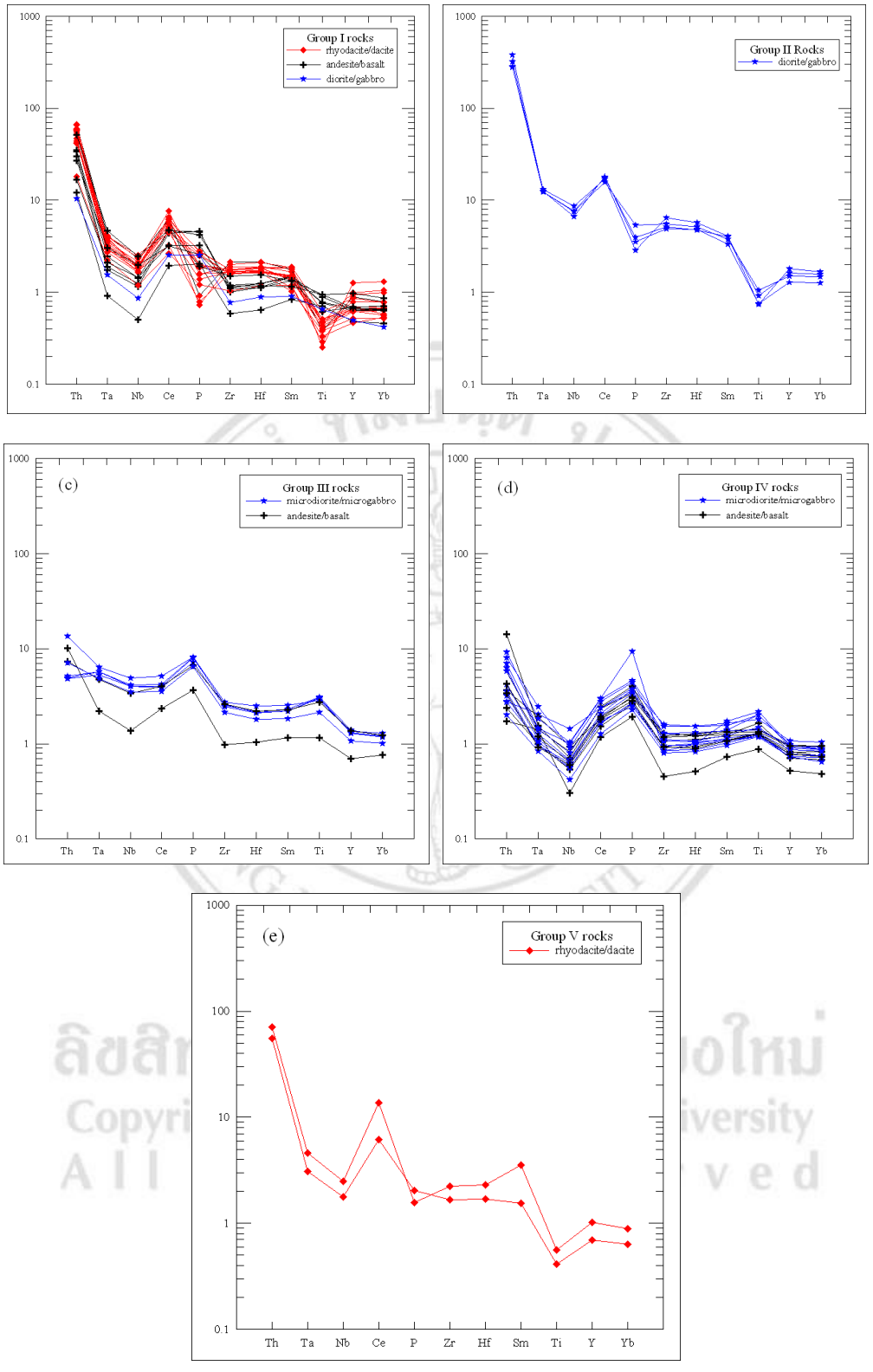

Figure 5.3 N - MORB - normalized patterns for the studied least-altered Group I (a), Group II (b), Group III (c), Group IV (d) and Group V (e) rocks. Normalizing values used are those of Sun and McDonough (1989).

5.2.1 Group I rocks

Group I rocks are composed of twenty three rock samples. The chemical compositions of the studied least-altered mafic to felsic volcanic/hypabyssal rocks are listed in Tables 5.1 and 5.2. This group can be separated into three subgroups by Zr/TiO_2-Nb/Y diagram of Winchester and Floyd (1977), and their textures as rhyodacite/dacite (KK-01, KK-04, KK-07, KK-08, KK-09, KK-11, KK-12, KK-13, KK-19, KK-21, KK-22, KK-23, TK-01, TK-03, TK-04 and TK-30), andesite/basalt (KK-14, KK-15, KK-17, KK-18, TK-12 and TK-23) and diorite/gabbro (NKT-093) that collected from the Tha Tako and Krok Phra areas, Nakhon Sawan province.

Group I rocks span the ranges in Zr/TiO_2 and Nb/Y from 0.01 to 0.08 and 0.09 to 0.33 respectively. Accordingly, they have similar chemical compositions, suggesting a common source rock or a common parental magma. They are compositionally classified as subalkalic rhyodacite/dacite and andesite/basalt on the Zr/TiO_2-Nb/Y diagram.

The FeO*/MgO variation diagrams for immobile major oxides and trace elements (Figure 5.4) of rhyodacite/dacite, andesite/basalt and diorite/gabbro show that the values for Nb, Zr and Y form broadly positive trends against FeO*/MgO, typical of incompatible element behavior. The trends for FeO*, TiO_2, MgO, P_2O_5, Ni, Cr, V and Sc descend relative to FeO*/MgO, recording the removal of mafic minerals and apatite. The pyroxene fractionation is in agreement with the occurrences of pyroxene phenocrysts/microphenocrysts in the studied samples (see Chapter 4).

The zirconium variation diagrams for least-mobile major oxide and trace elements (Figure 5.5) show that the values for Nb and Y are positive trends. The decreasing values for FeO*, TiO_2, P_2O_5, MgO, V, Ni, Sc and Cr in fractionated lavas indicated that the fractionation is controlled by the removal of mafic minerals and apatite.

Table 5.1 Whole-rock XRF major-element analyses of the studied least-altered Group I rocks recalculated to 100 wt% volatile-free, including loss on ignition and original analytical totals.

Sample number	KK-01	KK-04	KK-07	KK-08	KK-09	KK-11	KK-12	KK-13	KK-19
Rock type	Rhy	Rhy	Rhy	Rhy	Rhy	Rhy	Rhy	Rhy	Rhy
Area	TK	TK	TK	TK	TK	TK	TK	TK	TK
SiO_2	74.93	73.71	70.96	76.36	74.83	73.37	77.87	72.34	73.56
TiO_2	0.36	0.30	0.39	0.36	0.39	0.29	0.30	0.33	0.47
Al_2O_3	13.54	15.79	16.01	12.26	13.28	16.07	12.74	16.39	13.24
FeO*	2.50	2.44	2.97	2.67	3.11	3.35	2.13	2.24	3.97
MnO	0.01	0.03	0.01	0.03	0.03	0.05	0.01	0.02	0.07
MgO	0.13	0.44	0.60	0.23	0.42	0.25	0.42	0.51	1.13
CaO	1.40	1.38	1.96	1.48	1.14	0.45	1.00	1.76	1.72
Na_2O	3.47	3.51	3.69	3.67	3.61	3.15	3.35	3.73	3.53
K_2O	3.56	2.29	3.28	2.85	3.05	2.98	2.08	2.59	2.17
P_2O_5	0.097	0.10	0.14	0.08	0.13	0.05	0.09	0.10	0.14
LOI	1.31	3.01	2.98	1.74	2.01	2.26	2.60	2.89	3.49
Original Sum	100.34	99.64	100.29	99.55	99.89	100.26	100.20	100.37	99.94
FeO*/MgO	19.32	5.53	4.91	11.58	7.33	13.46	5.08	4.36	3.50

Sample no.	KK-21	KK-22	KK-23	TK-01	TK-03	TK-04	TK-30	KK-14	KK-15
Rock types	Rhy	Rhy	Rhy	Rhy	Rhy	Rhy	Rhy	And	And
Areas	TK	TK	TK	TK	TK	TK	TK	TK	TK
SiO_2	74.17	73.20	78.63	80.49	76.08	72.15	66.17	59.95	61.42
TiO_2	0.25	0.35	0.29	0.22	0.19	0.36	0.47	0.58	0.59
Al_2O_3	15.41	14.91	12.07	11.10	13.18	14.28	17.94	18.75	19.29
FeO*	2.02	2.84	1.60	2.77	3.38	5.12	5.03	6.61	6.40
MnO	0.03	0.03	0.01	0.03	0.05	0.03	0.08	0.08	0.15
MgO	0.55	1.02	0.37	0.20	0.26	0.97	1.59	2.94	2.42
CaO	1.21	1.21	0.31	0.89	1.13	3.00	3.41	5.25	4.31
Na_2O	3.11	3.03	2.15	3.31	3.65	2.81	2.89	3.46	3.18
K_2O	3.17	3.27	4.54	0.94	2.05	1.22	2.32	2.17	2.03
P_2O_5	0.08	0.13	0.04	0.06	0.04	0.07	0.10	0.23	0.21
LOI	2.59	2.69	0.90	1.03	0.73	0.89	2.27	2.74	3.48
Original Sum	99.61	99.74	100.42	100.19	99.93	99.31	99.97	99.92	100.01
FeO*/MgO	3.65	2.79	4.31	14.05	13.17	5.27	3.16	2.25	2.64

N.B.

FeO* = total iron as FeO and LOI = loss on ignition. TK = Tha Tako, and KP = Krok Phra. Rhy = rhyodacite/dacite, And = andesite/basalt, and Dio = diorite/gabbro.

Table 5.1 *(Continued)*

Sample number	KK-17	KK-18	TK-12	TK-23	NKT-093
Rock type	And	And	And	And	Dio
Area	TK	TK	TK	TK	KP
SiO_2	63.29	57.09	56.19	62.92	63.21
TiO_2	0.67	0.54	0.72	0.72	0.49
Al_2O_3	18.03	18.20	14.54	16.34	20.06
FeO*	7.72	7.55	6.77	8.20	4.76
MnO	0.10	0.10	0.14	0.12	0.01
MgO	2.21	4.91	3.53	3.13	2.67
CaO	2.70	7.78	13.28	5.26	3.74
Na_2O	4.21	2.59	1.92	2.44	3.45
K_2O	0.82	1.13	2.75	0.74	1.48
P_2O_5	0.24	0.10	0.17	0.13	0.13
LOI	3.28	3.96	1.39	0.92	4.24
Original Sum	99.74	100.13	99.90	100.43	99.80
FeO*/MgO	3.49	1.54	1.92	2.61	1.78

N.B.

FeO* = total iron as FeO and LOI = loss on ignition. TK = Tha Tako, and KP = Krok Phra. Rhy = rhyodacite/dacite, And = andesite/basalt, and Dio = diorite/gabbro.

Table 5.2 Low-abundance trace elements and REE compositions (in ppm) for the studied least-altered Group I rocks by ICP-MS analysis.

Sample number	KK-01	KK-04	KK-07	KK-08	KK-09	KK-11	KK-12	KK-13	KK-19
Rock type	Rhy	Rhy	Rhy	Rhy	Rhy	Rhy	Rhy	Rhy	Rhy
Area	TK	TK	TK	TK	TK	TK	TK	TK	TK
Sc	8.17	8.54	12.1	10.3	10.7	8.14	7.89	8.42	13.6
Ti	2168	2044	2735	2501	2449	2002	2042	2145	3020
V	16.9	37.6	60.7	30.2	29.6	13.0	30.4	36.1	91.7
Cr	1.96	3.53	2.69	2.06	5.75	1.91	5.82	4.26	4.93
Mn	385	591	540	450	406	513	405	484	810
Ni	0.75	1.21	0.89	0.73	0.97	0.40	1.02	0.86	2.69
Cu	4.27	2.71	3.37	27.8	3.36	4.81	22.9	2.80	7.85
Zn	24.9	41.2	44.8	39.1	40.1	34.0	63.9	59.2	91.2
Ga	10.6	10.1	12.4	9.55	11.2	13.7	11.6	12.4	15.7
Ge	0.60	0.64	1.01	1.14	0.80	0.78	0.81	0.75	0.78
Rb	76.5	49.2	82.7	66.3	66.3	84.6	44.9	72.0	54.8
Sr	68.8	90.9	103	127	91.1	143	76.2	94.6	153
Y	18.4	19.2	19.2	22.0	18.1	24.7	17.1	17.7	24.0
Zr	130	124	129	140	115	158	125	130	129
Nb	4.48	4.28	4.41	4.93	3.92	5.43	4.23	4.52	4.55
Cs	0.67	0.61	1.96	1.01	0.65	0.88	0.42	1.01	0.60
Ba	778	993	840	1067	750	700	722	652	833
La	19.2	24.3	23.7	33.8	20.5	29.2	25.0	26.4	26.9
Ce	37.3	41.6	46.9	57.2	38.3	47.1	44.2	49.2	46.4
Pr	4.84	5.42	5.78	7.04	5.10	6.30	5.49	5.84	6.51
Nd	18.8	20.8	22.8	26.5	20.4	24.9	20.8	21.1	26.0
Sm	3.56	3.79	4.38	4.74	3.93	4.68	3.64	3.65	4.99
Eu	0.76	0.84	0.99	0.99	0.90	1.03	0.77	0.81	1.19
Gd	3.18	3.39	3.69	3.99	3.37	4.18	2.87	2.96	4.42
Tb	0.52	0.53	0.59	0.69	0.56	0.69	0.49	0.49	0.69
Dy	3.14	3.01	3.38	3.93	3.27	3.88	2.85	2.94	3.80
Ho	0.70	0.65	0.76	0.85	0.73	0.84	0.64	0.65	0.85
Er	2.00	1.81	2.08	2.39	2.03	2.42	1.86	1.84	2.35
Tm	0.29	0.27	0.31	0.36	0.30	0.35	0.29	0.28	0.34
Yb	2.05	1.77	2.15	2.40	2.03	2.41	1.94	1.97	2.35
Lu	0.32	0.28	0.35	0.37	0.33	0.38	0.32	0.31	0.36
Hf	3.74	3.34	3.87	3.88	3.41	4.38	3.51	3.72	3.69
Ta	0.48	0.52	0.39	0.47	0.41	0.55	0.42	0.50	0.43
Pb	2.40	1.91	3.92	3.80	2.69	3.73	2.10	2.86	3.20
Th	6.30	6.25	6.64	6.86	5.61	7.83	7.09	7.18	6.96
U	1.73	1.66	1.77	1.99	1.35	2.16	1.91	1.88	1.91
Selected element ratios									
Zr/TiO_2	0.036	0.041	0.033	0.039	0.030	0.055	0.041	0.040	0.028
Nb/Y	0.243	0.223	0.230	0.224	0.217	0.220	0.247	0.255	0.189
Nb/Zr	0.03	0.03	0.03	0.04	0.03	0.03	0.03	0.03	0.04
Y/Zr	0.14	0.15	0.15	0.16	0.16	0.16	0.14	0.14	0.19
[La/Sm]cn	3.30	3.90	3.30	4.36	3.18	3.80	4.19	4.41	3.29
[Sm/Lu]cn	1.86	2.24	2.11	2.13	2.00	2.06	1.89	1.96	2.34

N. B.

TK = Tha Tako, and KP = Krok Phra. Rhy = rhyodacite/dacite, And = andesite/basalt, and Dio = diorite/gabbro.

Table 5.2 *(Continued)*

Sample number	KK-21	KK-22	KK-23	TK-01	TK-03	TK-04	TK-30	KK-14	KK-15
Rock type	Rhy	Rhy	Rhy	Rhy	Rhy	Rhy	Rhy	And	And
Area	TK	TK	TK	TK	TK	TK	TK	TK	TK
Sc	6.36	10.2	7.78	13.1	16.8	18.6	18.0	26.8	25.9
Ti	1789	2272	1896	1466	1299	2233	3266	4084	4136
V	38.4	49.9	31.1	10.2	8.38	92.4	102	206	204
Cr	5.03	3.68	6.92	7.60	7.71	11.2	6.79	24.0	20.1
Mn	507	554	355	575	839	1080	1077	1218	1661
Ni	0.91	1.67	0.64	0.99	0.64	3.03	2.61	11.1	9.83
Cu	2.17	35.0	37.0	41.9	1.52	2.02	14.1	82.6	84.5
Zn	54.2	57.2	53.2	44.2	49.7	71.4	102	85.4	143
Ga	11.4	12.4	6.72	11.1	17.2	15.6	15.6	18.2	19.1
Ge	0.86	0.66	1.60	1.16	0.98	1.98	1.08	1.39	1.50
Rb	80.9	71.3	103	27.2	55.2	28.9	88.3	53.6	54.2
Sr	221	112	118	61.2	77.3	188	247	511	603
Y	13.1	17.4	14.4	26.3	35.6	27.6	19.4	17.7	18.8
Zr	122	117	119	76.9	148	123	110	83.2	88.3
Nb	4.38	3.83	3.92	2.76	5.89	5.55	5.74	2.90	3.34
Cs	1.44	0.53	0.54	0.34	0.53	0.23	0.76	0.48	0.56
Ba	991	953	994	320	585	475	524	780	752
La	25.8	17.1	9.63	10.1	18.9	16.1	18.0	17.4	17.7
Ce	46.4	33.9	24.3	19.7	38.6	33.4	35.5	35.1	35.5
Pr	5.29	5.04	2.98	2.80	5.08	4.29	4.46	4.70	4.63
Nd	18.1	20.3	12.3	12.4	20.9	17.4	17.4	18.9	19.3
Sm	2.92	3.90	2.70	3.13	4.86	4.00	3.49	3.81	3.93
Eu	0.63	0.77	0.60	0.80	1.23	1.13	0.86	0.98	0.97
Gd	2.21	3.22	2.36	3.93	5.52	4.30	3.44	3.43	3.38
Tb	0.38	0.51	0.41	0.70	0.97	0.78	0.58	0.54	0.57
Dy	2.10	2.89	2.36	4.50	6.14	4.76	3.47	3.20	3.25
Ho	0.48	0.65	0.52	1.03	1.37	1.12	0.77	0.69	0.72
Er	1.43	1.71	1.49	2.96	3.97	3.02	2.13	1.98	1.97
Tm	0.22	0.26	0.22	0.45	0.60	0.48	0.32	0.29	0.29
Yb	1.63	1.71	1.57	3.01	3.99	3.21	2.16	1.94	1.94
Lu	0.27	0.26	0.26	0.46	0.62	0.50	0.34	0.30	0.31
Hf	3.54	3.47	3.30	2.42	4.30	3.48	3.15	2.56	2.55
Ta	0.46	0.36	0.39	0.30	0.54	0.53	0.62	0.25	0.32
Pb	2.89	2.54	1.68	8.02	9.31	6.07	22.0	8.18	10.8
Th	7.97	5.31	5.27	2.18	5.08	4.98	6.15	4.07	4.22
U	2.14	1.60	1.43	0.90	1.40	1.71	1.46	1.09	1.16
Selected element ratios									
Zr/TiO_2	0.048	0.033	0.041	0.035	0.077	0.034	0.024	0.014	0.015
Nb/Y	0.334	0.220	0.271	0.105	0.166	0.201	0.96	0.164	0.177
Nb/Zr	0.04	0.03	0.03	0.04	0.04	0.04	0.05	0.03	0.04
Y/Zr	0.11	0.15	0.12	0.34	0.24	0.22	0.18	0.21	0.21
[La/Sm]cn	5.38	2.68	2.18	1.97	2.37	2.46	3.14	2.78	2.74
[Sm/Lu]cn	1.82	2.48	1.75	1.15	1.31	1.33	1.71	2.12	2.12

N.B.

TK = Tha Tako, and KP = Krok Phra. Rhy = rhyodacite/dacite, And = andesite/basalt, and Dio = diorite/gabbro.

Table 5.2 *(Continued)*

Sample number	KK-17	KK-18	TK-12	TK-23	NKT-093
Rock type	And	And	And	And	Dio
Area	TK	TK	TK	TK	KP
Sc	28.2	35.6	27.6	29.5	12.5
Ti	4510	3635	4633	4794	2918
V	248	249	62.9	204	103
Cr	6.42	122	14.6	38.7	26.0
Mn	1304	1220	1630	1505	594
Ni	2.40	36.2	8.89	13.1	25.0
Cu	89.0	109	186	33.5	11.4
Zn	92.9	70.2	406	102	43.4
Ga	17.4	15.6	12.8	17.6	16.3
Ge	1.57	1.16	1.70	1.07	1.03
Rb	19.4	36.0	71.6	24.6	18.9
Sr	363	705	310	252	326
Y	18.0	13.5	27.1	18.8	13.8
Zr	74.0	43.5	81.7	86.8	57.1
Nb	2.70	1.17	3.38	4.60	1.99
Cs	1.26	1.32	6.04	1.23	0.94
Ba	322	312	908	248	236
La	15.9	6.80	12.0	11.1	8.85
Ce	33.1	14.6	24.3	23.8	19.0
Pr	4.43	2.01	3.49	3.13	2.57
Nd	18.9	9.1	15.4	12.9	10.8
Sm	3.90	2.21	3.55	3.03	2.35
Eu	1.05	0.71	1.00	0.90	0.66
Gd	3.53	2.38	4.03	3.20	2.30
Tb	0.57	0.39	0.68	0.57	0.39
Dy	3.29	2.38	4.19	3.39	2.23
Ho	0.73	0.55	0.98	0.75	0.47
Er	2.06	1.50	2.68	2.01	1.33
Tm	0.31	0.22	0.40	0.30	0.19
Yb	1.99	1.39	2.64	1.98	1.28
Lu	0.30	0.22	0.41	0.30	0.20
Hf	2.33	1.32	2.29	2.38	1.83
Ta	0.23	0.12	0.28	0.40	0.20
Pb	5.17	2.27	29.3	6.39	4.64
Th	3.61	1.45	2.00	3.24	1.25
U	1.00	0.43	0.68	0.67	0.46
Selected element ratios					
Zr/TiO_2	0.011	0.008	0.011	0.012	0.012
Nb/Y	0.150	0.086	0.125	0.244	0.144
Nb/Zr	0.04	0.03	0.04	0.05	0.03
Y/Zr	0.24	0.31	0.33	0.22	0.24
[La/Sm]cn	2.50	1.89	2.06	2.22	2.30
[Sm/Lu]cn	2.14	1.69	1.46	1.67	2.01

N.B.

TK = Tha Tako, and KP = Krok Phra. Rhy = rhyodacite/dacite, And = andesite/basalt, and Dio = diorite/gabbro.

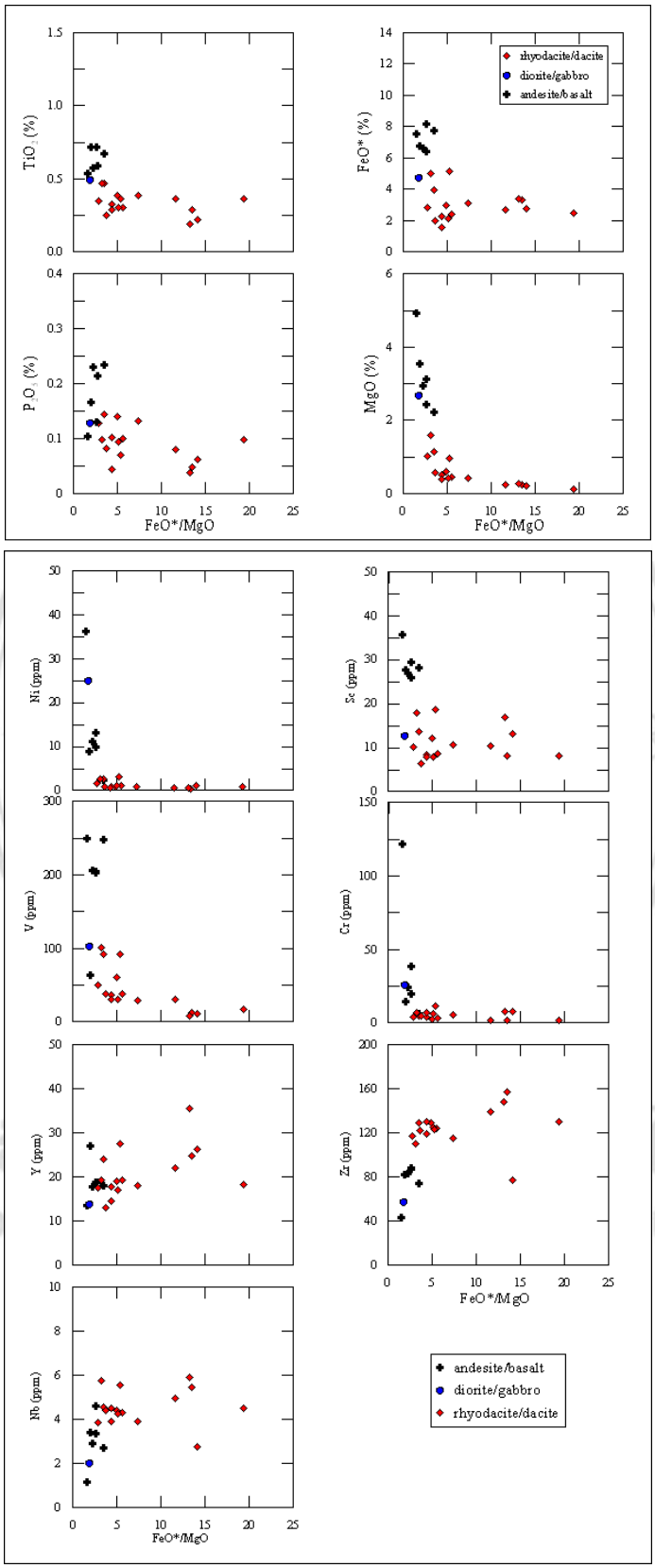

Figure 5.4 FeO*/MgO variation diagrams for immobile major and trace elements of the studied least-altered felsic to mafic volcanic/hypabassal Group I rocks.

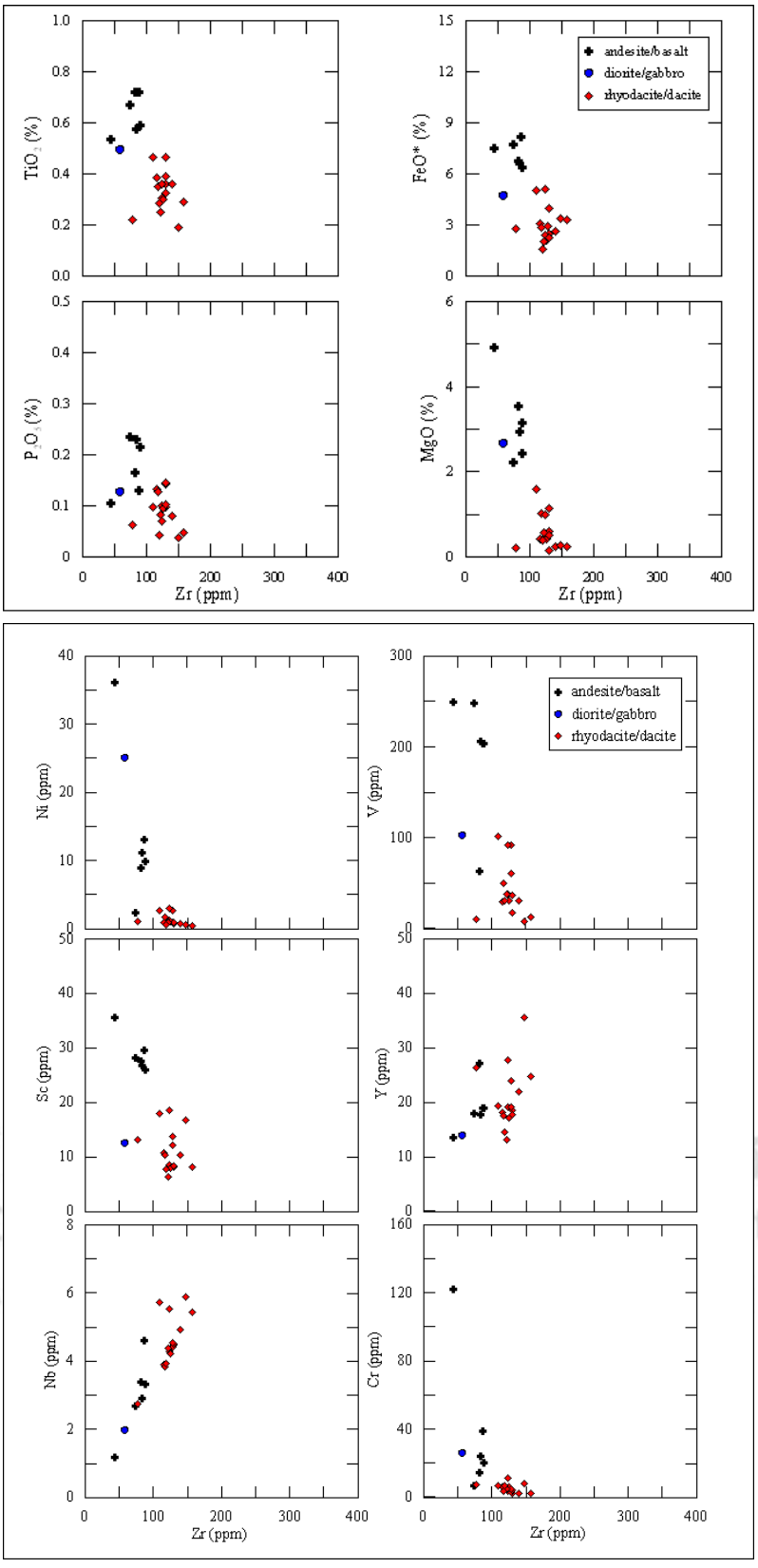

Figure 5.5 Zr variation diagrams for immobile major and trace elements of the studied least-altered felsic to mafic volcanic/hypabassal Group I rocks.

The relationships between incompatible-element pairs for the studied rhyodacite/dacite, andesite/basalt and diorite/gabbro rock samples in Group I rocks, such as Nb-Zr and Y-Zr, are linear, with ratios of Nb/Zr = 0.04 ± 0.007 and Y/Zr 0.20 ± 0.060. These signify that all the rocks are essentially co-magmatic. They might have formed by different degrees of partial melting of a common source rock or by different degrees of crystal fractionation of the same parental magma (Figure 5.5).

The studied rhyodacite/dacite, andesite/basalt and diorite/gabbro suite have chondrite-normalized values for La and Lu in ranges of 21.68 - 107.43 and 6.09 - 19.31, respectively. Their REE patterns (Figure 5.6) are typical of calc-alkalic rocks, i.e. LREE enrichment and relatively flat heavy REE (herein HREE), with chondrite-normalized La/Sm [herein (La/Sm)cn] and Sm/Lu [herein (Sm/Lu)cn] ranging from 1.89 to 5.38 and 1.15 to 2.48, respectively. The calc-alkalic nature is well supported by their positions on binary diagrams Ti-Zr and V-Ti and ternary diagrams Ti–Zr–Y, Hf–Th–Ta and Y–La–Nb, although the applied diagrams were designed for basalts (see section 5.3). The more pronounced negative Eu anomalies in the acid rocks relative to the basic rocks are due to plagioclase fractionation. The lower abundances for P in the acid rocks relative to the basic rocks are attributed to apatite fractionation. In terms of N-MORB normalized multi-element patterns (Figure 5.7), the rocks generally show flat patterns with negative Nb and Ta anomalies. This implies that the rhyodacite/dacite, andesite/basalt and diorite/gabbro have a subduction-related signature.

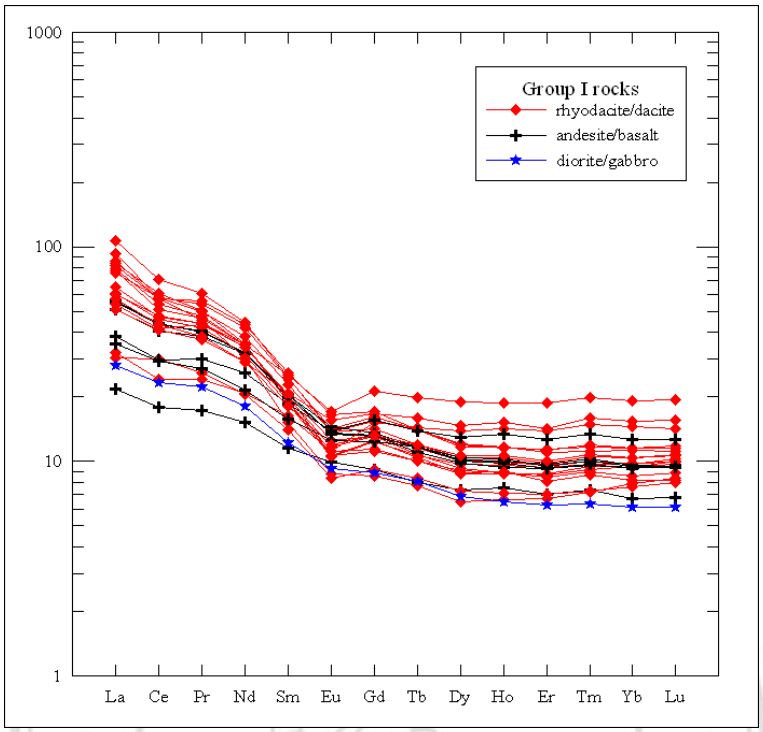

Figure 5.6 Chondrite-normalized REE patterns for the least-altered Group I rocks presented in this study. The normalizing values used are those of Taylor and Gorton (1977).

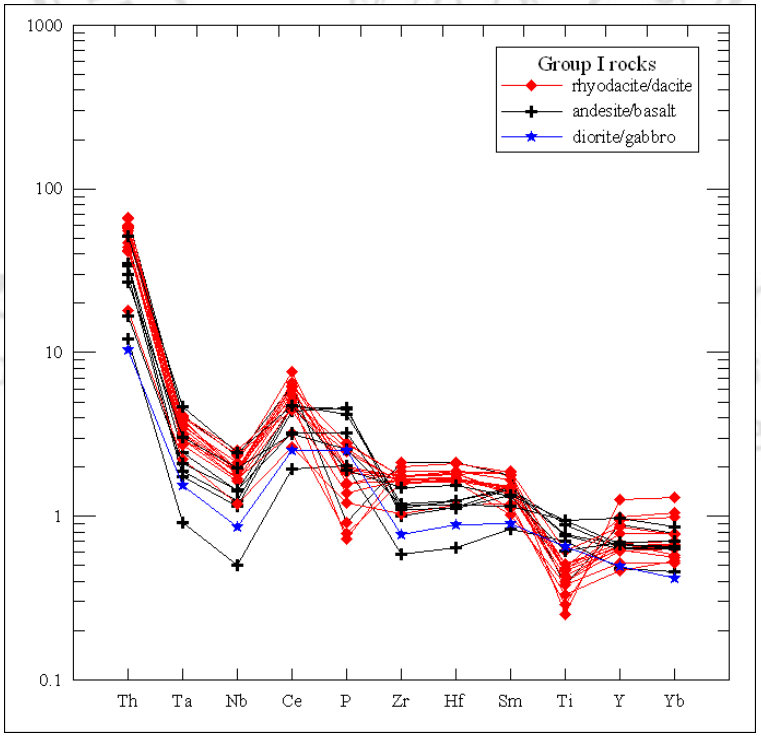

Figure 5.7 N - MORB - normalized patterns for the studied least-altered Group I rocks. The normalizing values used are those of Sun and McDonough (1989).

5.2.2 Group II rocks

Group II rocks are composed of four rock samples (LS-020, LS-021, LS-03 and LS-05) that were collected from the Chum Ta Bong area, Uthai Thani province. They are nomenclatured as rhyodacite/dacite by the Zr/TiO_2-Nb/Y diagram of Winchester and Floyd (1977), but as diorite/gabbro by their textures and minerals. The chemical compositions of the studied least-altered mafic hypabyssal rocks are listed in Tables 5.3 and 5.4.

Group II rocks span the narrow ranges in Zr/TiO_2 and Nb/Y from 0.05 to 0.09 and 0.39 to 0.43, respectively. Accordingly, they are likely to have a common source rock or common parental magma. They have a subalkalic affinity on the Zr/TiO_2-Nb/Y diagram.

The FeO*/MgO variation diagrams for immobile major oxides and trace elements (Figure 5.8) of diorite show that the values for Nb, Zr and Y form broadly positive trends, typical of incompatible element behavior. The values for FeO*, TiO_2, MgO, P_2O_5, Ni, Cr, V and Sc descend with increasing FeO*/MgO, recording the removals of mafic minerals and apatite. The pyroxene fractionation is in agreement with the occurrences of pyroxene phenocrysts/microphenocrysts in the studied samples (see Chapter 4).

The zirconium variation diagrams for least-mobile major oxide and trace elements (Figure 5.9) show that the values for Nb and Y form positive trends that can be traced back to zero. The relationships between incompatible-element pairs are linear, with ratios of Nb/Zr = 0.04 ± 0.005 and Y/Zr 0.11 ± 0.010. These signify that all the rocks are essentially co-genetic. They might have been formed by different degrees of partial melting of a common source rock or by different degrees of crystal fractionation of the same parental magma.

The studied diorite/gabbro have chondrite-normalized values for La and Lu in ranges of 180 - 218 and 17.9 – 24.2, respectively. Their REE patterns (Figure 5.10) are typical of calc-alkalic rocks, i.e. LREE enrichment and relatively flat HREE, with (La/Sm)cn and (Sm/Lu)cn ranging from 3.24 to

4.79 and 2.29 to 2.54, respectively. Their N-MORB normalized multi-element patterns (Figure 5.11) generally show negative Nb and Ta anomalies. This suggests that the diorite/gabbro has a subduction-related signature. The calc-alkalic nature is well supported by their positions on ternary diagrams Hf–Th–Ta and Y–La–Nb, although the applied diagrams were designed for basalts (see section 5.3).

Table 5.3 Whole-rock XRF major-element analyses of the studied least-altered Group II rocks recalculated to 100 wt% volatile-free, including loss on ignition and original analytical totals.

Sample number	LS-020	LS-021	LS-03	LS-05
Rock type	Dio	Dio	Dio	Dio
Area	CB	CB	CB	CB
SiO_2	70.54	69.28	73.02	64.48
TiO_2	0.69	0.57	0.56	0.80
Al_2O_3	13.68	15.75	13.54	16.57
FeO*	4.72	3.54	3.56	5.13
MnO	0.01	0.02	0.01	0.06
MgO	1.11	0.99	0.45	1.92
CaO	2.94	2.59	2.19	3.74
Na_2O	2.47	2.94	2.52	3.58
K_2O	3.64	4.12	4.01	3.46
P_2O_5	0.20	0.18	0.15	0.27
LOI	0.67	0.71	0.61	0.43
Original Sum	100.07	100.08	100.27	99.62
FeO*/MgO	4.23	3.57	7.84	2.68

N.B.

FeO* = total iron as FeO and LOI = loss on ignition. CB = Chum Ta Bong, and Dio = diorite/gabbro.

Table 5.4 Low-abundance trace elements and REE compositions (in ppm) for the studied least-altered Group II rocks by ICP-MS analysis.

Sample number	LS-020	LS-021	LS-03	LS-05
Rock type	Dio	Dio	Dio	Dio
Area	CB	CB	CB	CB
Sc	13.7	10.8	13.0	16.1
Ti	4640	3847	3932	5546
V	67.0	53.6	38.6	87.6
Cr	17.2	14.6	8.91	34.9
Mn	731	532	628	863
Ni	5.74	5.43	2.82	14.6
Cu	9.95	6.53	3.79	10.7
Zn	92.0	75.3	69.1	97.7
Ga	20.1	19.7	21.2	20.5
Ge	1.67	1.44	1.65	1.57
Rb	226	222	225	203
Sr	256	268	223	317
Y	45.0	35.8	50.4	42.0
Zr	376	361	478	408
Nb	17.7	15.5	20.1	17.4
Cs	13.1	7.90	5.78	9.69
Ba	945	976	1158	996
La	61.2	68.8	56.7	55.2
Ce	130	134	126	118
Pr	15.3	14.9	15.5	13.7
Nd	56.4	52.2	59.2	52.3
Sm	10.4	8.75	10.7	9.92
Eu	1.62	1.43	1.69	1.74
Gd	8.51	6.88	8.84	8.05
Tb	1.47	1.13	1.53	1.38
Dy	8.19	6.46	8.66	7.66
Ho	1.74	1.39	1.83	1.69
Er	4.93	3.86	5.10	4.55
Tm	0.72	0.56	0.76	0.67
Yb	4.77	3.85	5.09	4.46
Lu	0.73	0.57	0.78	0.68
Hf	9.69	9.93	11.7	10.4
Ta	1.62	1.66	1.74	1.62
Pb	41.3	29.2	31.1	36.5
Th	38.6	45.5	33.5	33.9
U	8.94	9.03	5.83	7.37
Selected element ratios				
Zr/TiO_2	0.054	0.063	0.086	0.051
Nb/Y	0.394	0.432	0.399	0.415
Nb/Zr	0.05	0.04	0.04	0.04
Y/Zr	0.12	0.10	0.11	0.10
[La/Sm]cn	3.57	4.79	3.24	3.39
[Sm/Lu]cn	2.39	2.54	2.29	2.43

N.B.

CB = Chum Ta Bong, and Dio = diorite/gabbro.

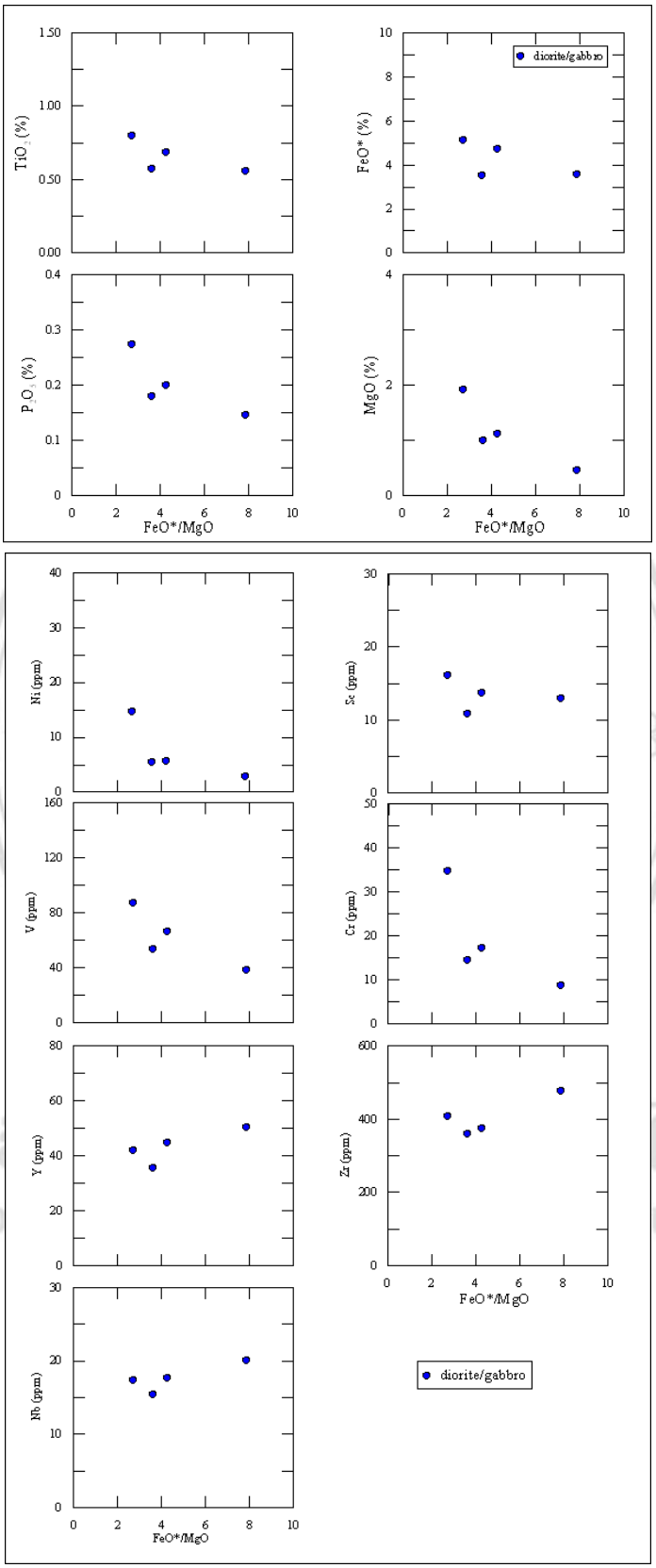

Figure 5.8 FeO*/MgO variation diagrams for immobile major and trace elements of the studied least-altered mafic hypabassal Group II rocks.

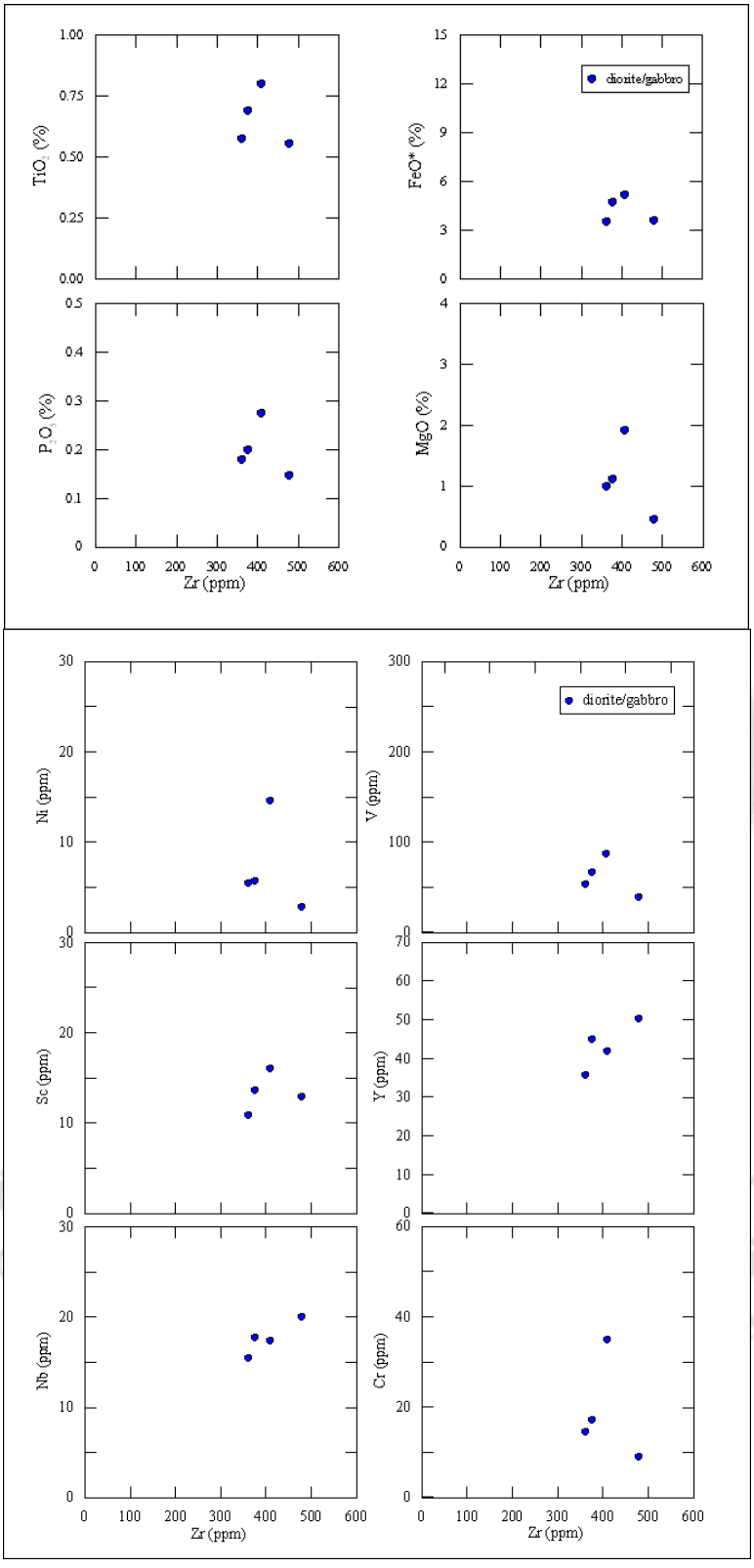

Figure 5.9 Zr variation diagrams for immobile major and trace elements of the studied least-altered mafic hypabassal Group II rocks.

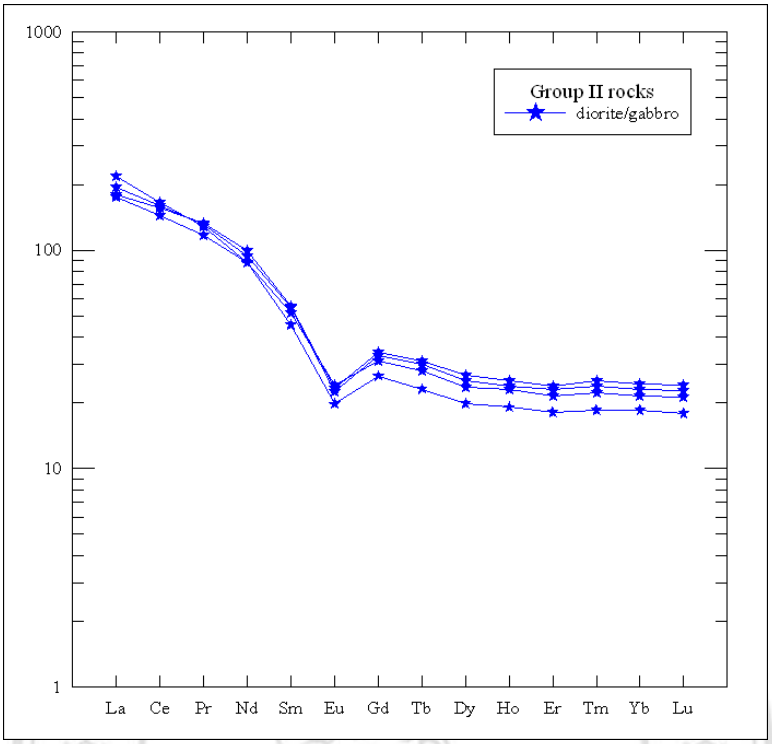

Figure 5.10 Chondrite-normalized REE patterns for the least-altered Group II rocks presented in this study. The normalizing values used are those of Taylor and Gorton (1977).

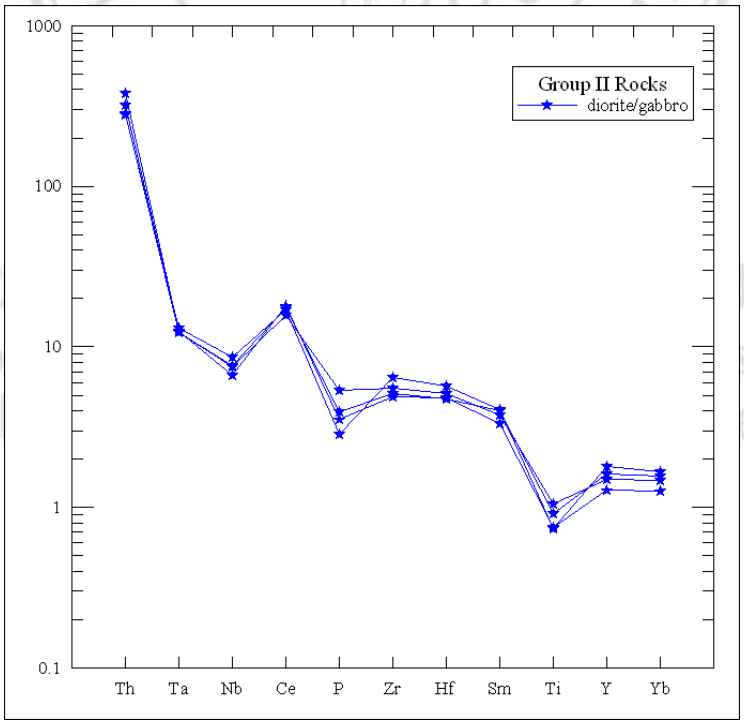

Figure 5.11 N - MORB - normalized patterns for the studied least-altered Group II rocks. Normalizing value used are those of Sun and McDonough (1989).

5.2.3 Group III rocks

Group III rocks have seven samples that are composed of microdiorite/microgabbro (KK-16, TK-07, TK-13, TK-15 and TK-25) and andesite/basalt (TK-14 and TK-20) that were collected from Tha Tako, Nakhon Sawan Province. The given nomenclatures are based on the Zr/TiO_2-Nb/Y diagram of Winchester and Floyd (1977) and their textures. The chemical compositions of the studied least-altered Group III mafic rocks were listed in Tables 5.5 and 5.6.

Group III rocks span the ranges in Zr/TiO_2 and Nb/Y from 0.009-0.010 and 0.16 to 0.30 respectively. They are classified as subalkalic andesite/basalt on the Zr/TiO_2-Nb/Y diagram. Both of the Group III volcanic and hypabyssal rock samples have similar chemical compositions suggesting either a common source rock or common parental magma.

The FeO*/MgO variation diagrams for immobile major oxides and trace elements (Figure 5.12) of Group III andesite/basalt and diorite/gabbro show that the values for FeO*, TiO_2, P_2O_5, Nb, Zr, and Y form broadly positive trends, typical of incompatible element behavior. The trends for MgO, Ni, and Sc descend relative to FeO*/MgO, recording olivine, pyroxene and chrome-spinel removals. The pyroxene fractionation is in agreement with the occurrences of pyroxene phenocrysts/microphenocrysts in the studied samples (see Chapter 4).

The zirconium variation diagrams for least-mobile major oxide and trace elements (Figure 5.13) show that the values for TiO_2, FeO*, P_2O_5, V, Nb and Y form positive trends. The increasing TiO_2, FeO* and V with increasing Zr values indicated that the Group III rocks are tholeiitic series.

Table 5.5 Whole-rock XRF major-element analyses of the studied least-altered Group III rocks recalculated to 100 wt% volatile-free, including loss on ignition and original analytical totals.

Sample number	KK-16	TK-07	TK-13	TK-15	TK-25	TK-14	TK-20
Rock type	Dio	Dio	Dio	Dio	Dio	And	And
Area	TK	TK	TK	TK	TK	TK	TK
SiO_2	54.89	51.02	50.13	49.70	51.87	52.26	55.51
TiO_2	2.19	2.29	2.36	2.33	1.63	0.88	2.08
Al_2O_3	15.39	16.90	18.00	18.74	17.28	11.76	15.79
FeO*	11.31	11.57	11.48	11.10	9.26	8.24	10.25
MnO	0.13	0.20	0.20	0.23	0.19	0.43	0.05
MgO	5.30	5.81	5.85	6.13	6.42	5.50	5.28
CaO	6.65	9.07	8.64	8.24	9.52	18.39	7.62
Na_2O	2.94	2.17	2.33	2.34	3.13	1.48	2.50
K_2O	0.79	0.60	0.59	0.78	0.36	0.88	0.57
P_2O_5	0.42	0.37	0.41	0.41	0.33	0.19	0.34
LOI	2.85	1.30	1.27	2.17	1.36	0.61	1.46
Original Sum	99.81	100.22	99.80	100.37	99.82	100.03	100.44
FeO*/MgO	2.13	1.99	1.96	1.81	1.44	1.50	1.94

N.B.

FeO* = total iron as FeO and LOI = loss on ignition. TK = Tha Tako, And = andesite/basalt, and Dio = diorite/gabbro.

Table 5.6 Low-abundance trace elements and REE compositions (in ppm) for the studied least-altered Group III rocks by ICP-MS analysis.

Sample number	KK-16	TK-07	TK-13	TK-15	TK-25	TK-14	TK-20
Rock type	Dio	Dio	Dio	Dio	Dio	And	And
Area	TK	TK	TK	TK	TK	TK	TK
Sc	35.7	37.9	38.5	37.8	35.0	40.5	35.9
Ti	14199	14255	15010	14661	10074	6084	14093
V	319	315	330	314	241	391	313
Cr	67.3	147	141	145	172	23.1	146
Mn	1565	1899	1984	2330	1879	4356	1845
Ni	46.0	62.9	55.0	61.2	57.1	18.2	56.5
Cu	60.5	60.5	64.0	45.3	72.1	5.42	69.0
Zn	118	159	156	148	121	265	116
Ga	19.7	19.1	19.9	18.8	16.8	10.6	18.5
Ge	1.49	1.63	1.68	1.36	1.58	1.98	1.64
Rb	22.8	21.2	18.2	27.8	11.8	39.1	32.5
Sr	426	292	283	278	568	133	296
Y	37.7	36.2	39.1	36.8	30.0	19.6	38.6
Zr	204	181	189	191	158	72.5	192
Nb	11.4	9.42	9.63	9.37	8.10	3.19	7.94
Cs	0.68	0.83	0.70	0.60	0.67	2.65	1.59
Ba	216	114	117	104	49.8	167	116
La	16.8	11.3	12.1	11.7	10.6	7.13	11.7
Ce	38.7	29.1	31.7	30.3	26.7	17.7	30.0
Pr	5.89	4.59	4.89	4.71	3.98	2.61	4.55
Nd	27.1	21.8	23.3	22.9	18.6	12.2	22.0
Sm	6.67	5.81	6.12	5.84	4.81	3.04	5.96
Eu	2.24	1.99	2.15	2.06	1.63	0.95	2.01
Gd	7.56	6.68	7.19	6.90	5.51	3.52	6.94
Tb	1.27	1.15	1.20	1.20	0.95	0.61	1.17
Dy	7.35	6.89	7.01	6.99	5.50	3.79	7.06
Ho	1.63	1.46	1.53	1.52	1.26	0.84	1.52
Er	4.42	3.96	4.13	4.04	3.24	2.30	4.11
Tm	0.62	0.57	0.59	0.56	0.47	0.35	0.59
Yb	3.94	3.59	3.68	3.63	3.07	2.33	3.74
Lu	0.60	0.53	0.57	0.53	0.45	0.37	0.57
Hf	5.11	4.32	4.47	4.38	3.70	2.13	4.54
Ta	0.84	0.70	0.75	0.76	0.64	0.29	0.63
Pb	3.37	15.8	7.49	7.64	9.79	8.60	10.2
Th	1.63	0.58	0.62	0.59	0.85	1.22	0.88
U	0.48	0.18	0.20	0.20	0.28	10.5	0.30
Selected element ratios							
Zr/TiO_2	0.009	0.008	0.008	0.008	0.010	0.008	0.009
Nb/Y	0.302	0.260	0.246	0.255	0.270	0.163	0.206
Nb/Zr	0.06	0.05	0.05	0.05	0.05	0.04	0.04
Y/Zr	0.18	0.20	0.21	0.19	0.19	0.27	0.20
[La/Sm]cn	1.54	1.18	1.20	1.22	1.34	1.43	1.20
[Sm/Lu]cn	1.84	1.81	1.79	1.85	1.77	1.38	1.74

N.B.

TK = Tha Tako, And = andesite/basalt, and Dio = diorite/gabbro.

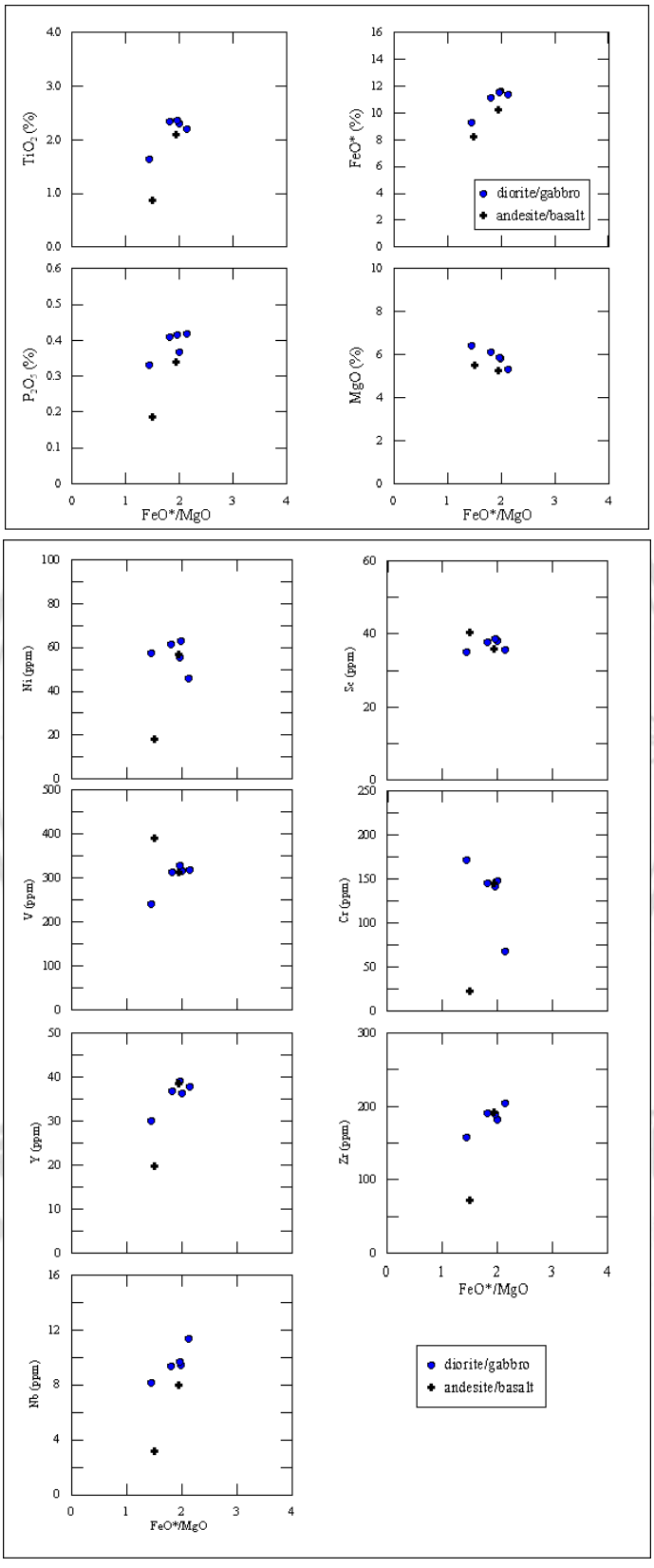

Figure 5.12 FeO*/MgO variation diagrams for immobile major and trace elements of the studied least-altered, Group III mafic hypabassal rocks.

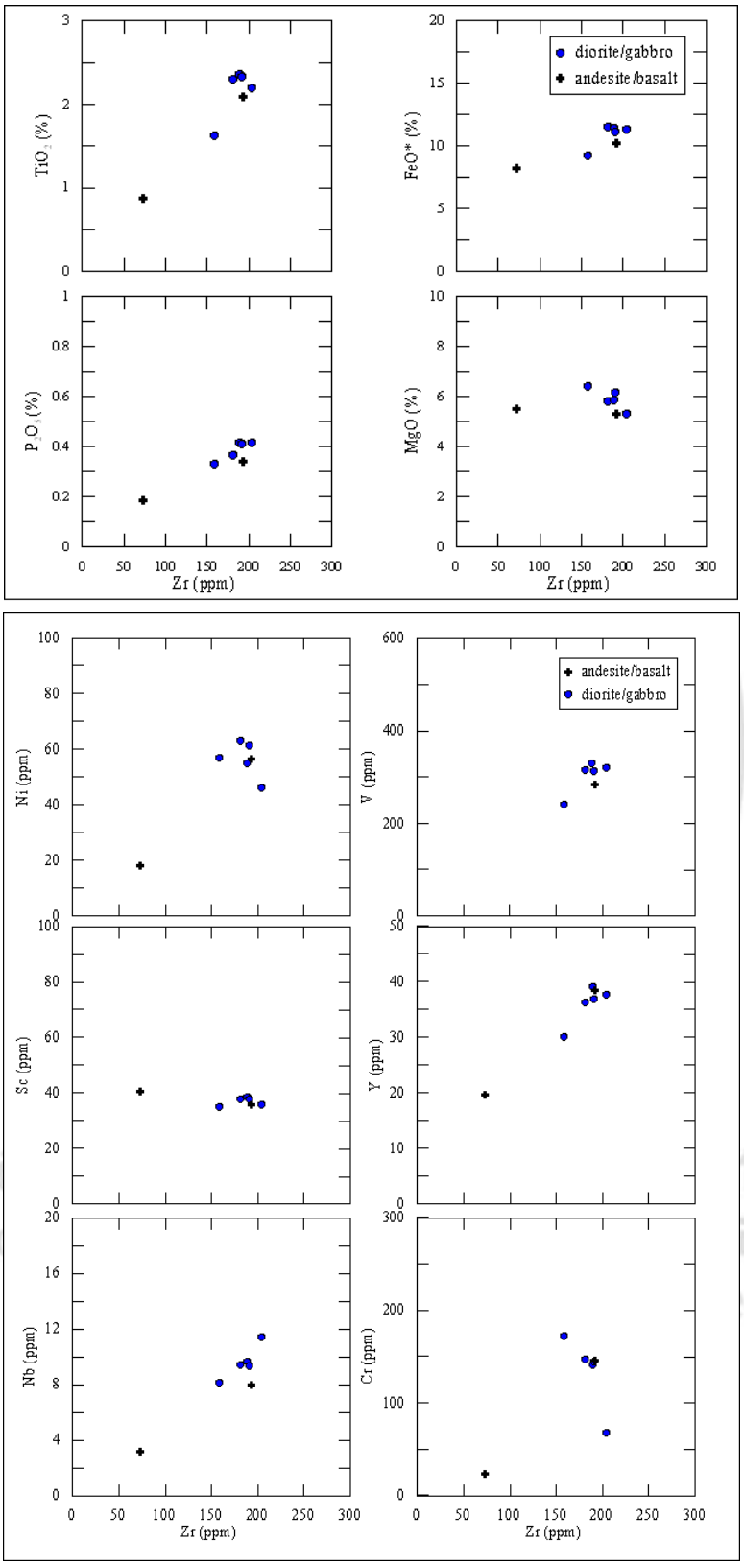

Figure 5.13 Zr variation diagrams for immobile major and trace elements of the studied least-altered, Group III felsic to mafic volcanic/hypabassal rocks.

The relationships between incompatible-element pairs for the studied Group III mafic volcanic/hypabassal rock samples, such as Nb-Zr and Y-Zr (Figure 5.13), are linear, with Nb/Zr = 0.048 ± 0.007 and Y/Zr = 0.206 ± 0.030. These signify that all the rocks are essentially co-genetic. They might have been formed by different degrees of partial melting of a common source rock or by different degrees of crystal fractionation of the same parental magma. The former is unlikely as the patterns for the incompatible-element pairs do not trace back to zero.

The studied subalkalic andesite/basalt suite have chondrite-normalized values for La and Lu in ranges of 22.6 - 53.4 and 11.5 - 18.8, respectively. Their REE patterns (Figure 5.14) are typical of tholeiitic rocks, i.e. slightly LREE enriched patterns, with (La/Sm)cn and (Sm/Lu)cn ranging from 1.18 to 1.53 and 1.38 to 1.85, respectively. In terms of N-MORB normalized multi-element patterns (Figure 5.15), the rocks generally show relatively flat patterns with negative niobium anomalies. These indicate that the subalkalic andesite/basalt have been crystallized from MORB-like magma that contain a crustal signature. The tholeiitic nature is well supported by their positions on ternary diagrams Ti–Zr–Y, Hf–Th–Ta and Y-La-Nb, although the applied diagrams were designed for basalts (see section 5.3).

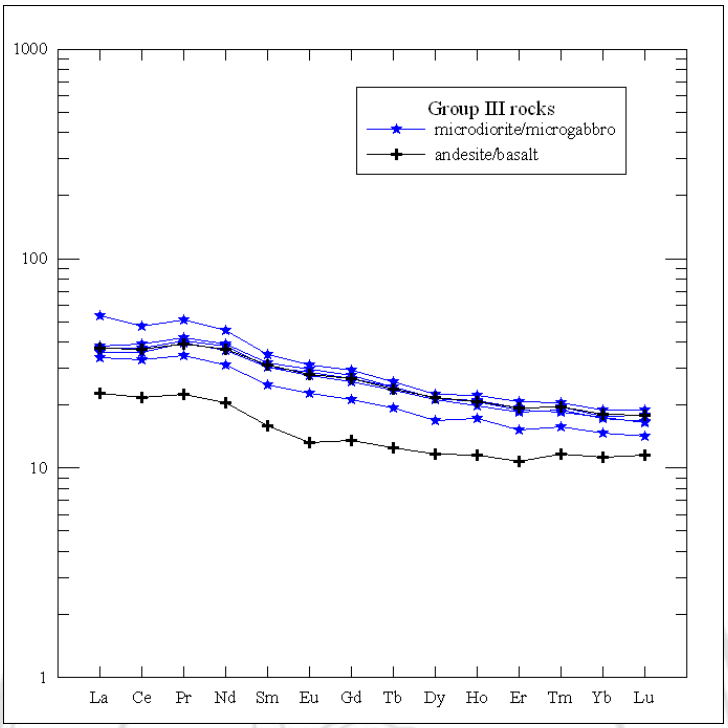

Figure 5.14 Chondrite-normalized REE patterns for the least-altered Group III rocks presented in this study. The normalizing values used are those of Taylor and Gorton (1977).

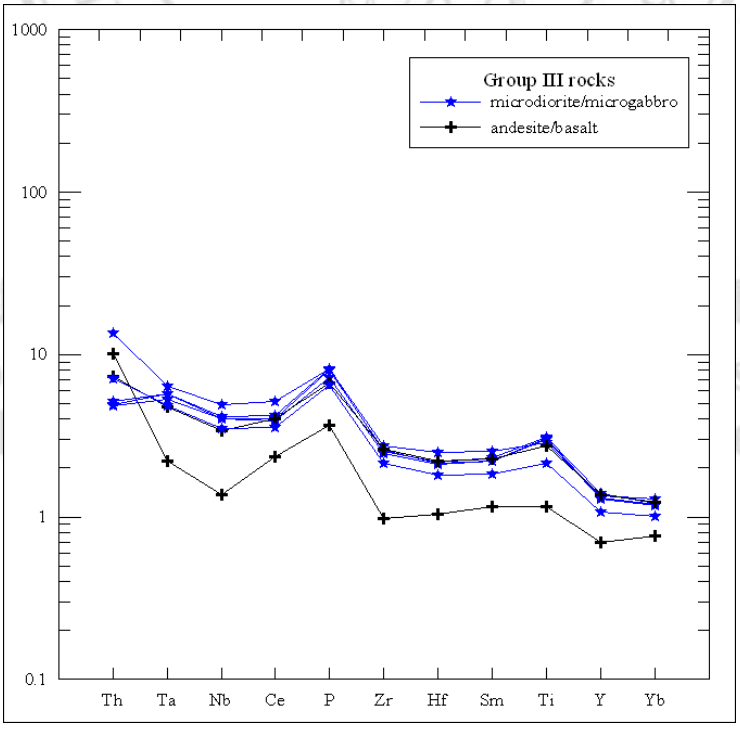

Figure 5.15 N - MORB - normalized patterns for the studied least-altered Group III rocks. Normalizing values used are those of Sun and McDonough (1989).

5.2.4 Group IV rocks

Group IV rocks have eighteen samples that are composed almost totally of microdiorite/microgabbro (TK-08, NKT-022, NKT-032, NKT-033, NKT-042, NKT-061, NKT-072, NKT-082, NKT-091, NKT-092, and NKT-111) and andesite/basalt (TK-26, TK-27, TK-37, NKT-031, NKT-051, NKT-101 and NKT-112). These are on the basis of Zr/TiO_2-Nb/Y diagram of Winchester and Floyd (1977) and their textures, and are from the Tha Tako and Krok Pra areas, Nakhon Sawan Province. The chemical compositions of the studied least-altered, Group IV mafic hypabyssal and volcanic rocks are listed in Tables 5.7 and 5.8.

Group IV rocks span the ranges in Zr/TiO_2 and Nb/Y from 0.004 to 0.009 and 0.05 to 0.12, respectively. Both of the volcanic and hypabyssal rock samples have similar chemical compositions suggesting either a common source rock or a common parental magma. They are classified as subalkalic andesite/basalt, using the Zr/TiO_2-Nb/Y diagram.

The FeO*/MgO variation diagrams for immobile major oxides and trace elements (Figure 5.16) of Group IV andesite/basalt and diorite/gabbro show that the values for FeO*, TiO_2, P_2O_5, V and Y form broadly positive trends, typical of incompatible element behavior. The trends for MgO, Ni and Cr descend with increasing FeO*/MgO values, recording removals of mafic minerals. The pyroxene fractionation is in agreement with the occurrences of pyroxene phenocrysts/microphenocrysts in the studied samples (see Chapter 4).

The zirconium variation diagrams for least-mobile major oxide and trace elements (Figure 5.17) show that the values for TiO_2, FeO*, P_2O_5, V, Nb and Y form positive trends. The increase in TiO_2, FeO* and V with increasing Zr values signifies that the Group IV rocks are tholeiitic series.

Table 5.7 Whole-rock XRF major-element analyses of the studied least-altered Group IV rocks recalculated to 100 wt% volatile-free, including loss on ignition and original analytical totals.

Sample number	TK-08	NKT-022	NKT-032	NKT-033	NKT-042	NKT-061	NKT-072	NKT-082	NKT-091
Rock type	Dio	Dio	Dio	Dio	Dio	Dio	Dio	Dio	Dio
Area	TK	KP	KP	KP	KP	KP	KP	KP	KP
SiO_2	53.34	55.47	61.74	55.72	58.71	55.73	55.97	60.61	60.89
TiO_2	1.52	1.52	1.05	1.13	0.90	0.93	1.66	1.38	0.98
Al_2O_3	17.94	17.92	15.87	19.01	15.88	18.55	18.60	15.96	14.99
FeO*	10.11	11.54	8.98	9.59	8.55	8.72	10.05	9.47	8.87
MnO	0.15	0.10	0.09	0.08	0.08	0.06	0.07	0.10	0.06
MgO	6.04	4.11	4.24	4.31	5.29	5.70	3.56	4.13	5.00
CaO	8.19	6.11	4.28	5.87	7.54	6.68	5.35	4.93	6.35
Na_2O	2.07	2.96	3.34	3.85	2.58	3.37	3.51	2.97	2.63
K_2O	0.44	0.03	0.23	0.25	0.35	0.12	0.75	0.22	0.08
P_2O_5	0.20	0.23	0.18	0.17	0.12	0.14	0.48	0.24	0.14
LOI	1.71	3.96	2.94	3.46	3.20	4.05	1.84	3.86	3.63
Original Sum	100.47	100.46	100.37	100.07	100.32	100.28	99.70	99.86	100.13
FeO*/MgO	1.67	2.81	2.12	2.22	1.61	1.53	2.82	2.29	1.77

Sample number	NKT-092	NKT-111	TK-26	TK-27	TK-37	NKT-031	NKT-051	NKT-101	NKT-112
Rock type	Dio	Dio	And	And	And	And	And	And	And
Area	KP	KP	TK	TK	TK	KP	KP	KP	KP
SiO_2	63.63	56.53	55.24	52.69	58.87	58.03	57.97	60.74	54.97
TiO_2	0.89	0.94	0.67	1.25	0.96	1.08	0.97	1.01	0.97
Al_2O_3	16.58	19.05	20.50	18.87	17.01	17.78	17.61	15.98	19.08
FeO*	6.59	8.66	8.65	8.70	9.15	8.83	8.72	8.30	8.95
MnO	0.03	0.02	0.13	0.12	0.10	0.09	0.07	0.01	0.06
MgO	3.41	5.48	4.59	6.08	3.10	4.39	4.97	4.28	5.46
CaO	5.13	5.70	7.37	9.75	8.43	5.78	6.49	6.16	6.66
Na_2O	3.49	3.43	2.59	2.23	1.51	3.66	2.98	3.11	3.55
K_2O	0.06	0.07	0.17	0.15	0.67	0.19	0.09	0.24	0.16
P_2O_5	0.19	0.13	0.10	0.16	0.20	0.17	0.13	0.15	0.14
LOI	3.28	3.11	0.67	1.40	1.17	1.99	2.84	3.14	3.15
Original Sum	100.34	99.67	100.18	99.89	99.73	99.82	99.86	100.18	99.72
FeO*/MgO	1.93	1.58	1.89	1.43	2.95	2.01	1.75	1.94	1.64

N.B.

FeO* = total iron as FeO and LOI = loss on ignition. TK = Tha Tako, KP = Krok Phra, Rhy = rhyodacite/dacite, And = andesite/basalt, and Dio = diorite/gabbro.

Table 5.8 Low-abundance trace elements and REE composition (in ppm) for the studied least-altered Group IV rocks by ICP-MS analysis.

Sample number	TK-08	NKT-022	NKT-032	NKT-033	NKT-042	NKT-061	NKT-072	NKT-082	NKT-091
Rock type	Dio	Dio	Dio	Dio	Dio	Dio	Dio	Dio	Dio
Area	TK	KP	KP	KP	KP	KP	KP	KP	KP
Sc	30.8	34.6	32.4	34.7	39.0	36.5	32.3	30.1	38.0
Ti	9588	9115	7083	7141	5710	6123	11678	8579	6402
V	273	412	264	295	246	268	314	308	253
Cr	74.7	5.03	13.5	18.3	84.4	62.3	4.59	14.9	30.0
Mn	1451	1215	1401	1254	1239	1172	1461	1343	1394
Ni	67.6	5.41	14.5	12.5	31.8	25.1	7.15	7.32	27.0
Cu	62.0	43.2	89.4	72.9	116	80.2	66.1	89.5	109
Zn	95.8	105	95.7	93.4	70.5	81.7	112	117	88.4
Ga	19.5	19.0	18.3	18.3	17.0	16.6	19.7	18.6	17.2
Ge	1.43	1.15	1.22	1.37	1.54	1.21	1.27	1.20	1.23
Rb	10.6	0.27	2.56	1.55	4.34	1.21	10.84	1.21	0.83
Sr	273	494	338	417	374	290	361	351	279
Y	27.0	26.2	26.8	25.3	21.6	20.3	27.3	30.1	24.2
Zr	118	93.7	95.7	82.1	59.4	62.8	62.3	112	70.3
Nb	3.35	2.12	1.86	1.54	0.98	1.30	2.44	2.34	1.31
Cs	0.83	0.01	0.18	0.09	0.30	0.07	0.44	0.04	0.05
Ba	50.0	25.9	98.2	115	63.0	44.0	136	69.5	70.5
La	6.28	8.83	7.21	5.75	3.63	5.14	8.89	8.91	4.62
Ce	17.9	20.7	17.8	14.6	9.52	12.5	22.5	22.0	12.4
Pr	2.87	3.14	2.79	2.35	1.64	2.04	3.50	3.47	2.05
Nd	14.9	14.8	13.4	11.7	8.60	9.96	17.2	16.5	10.5
Sm	4.10	3.65	3.61	3.22	2.54	2.71	4.53	4.31	3.01
Eu	1.50	1.33	1.25	1.18	1.01	1.02	1.56	1.49	1.11
Gd	4.98	4.29	4.20	4.04	3.36	3.39	5.28	5.05	3.86
Tb	0.87	0.75	0.75	0.71	0.61	0.60	0.89	0.88	0.69
Dy	5.15	4.59	4.57	4.43	3.83	3.68	5.19	5.37	4.34
Ho	1.14	1.02	1.03	1.00	0.86	0.84	1.13	1.20	0.95
Er	3.05	2.86	2.91	2.81	2.40	2.30	2.96	3.34	2.70
Tm	0.43	0.40	0.43	0.39	0.34	0.32	0.42	0.49	0.39
Yb	2.79	2.69	2.84	2.62	2.27	2.20	2.68	3.20	2.56
Lu	0.42	0.41	0.44	0.40	0.34	0.33	0.41	0.50	0.39
Hf	3.12	2.58	2.69	2.21	1.69	1.77	2.04	3.15	2.06
Ta	0.27	0.32	0.19	0.15	0.11	0.13	0.24	0.19	0.14
Pb	3.65	6.37	3.51	5.07	2.49	2.19	2.78	3.50	3.61
Th	0.33	0.96	0.70	0.51	0.24	0.38	1.11	0.84	0.33
U	0.15	0.35	0.27	0.20	0.10	0.14	0.39	0.35	0.14
Selected element ratios									
Zr/TiO_2	0.008	0.006	0.009	0.007	0.007	0.007	0.004	0.008	0.007
Nb/Y	0.124	0.081	0.069	0.061	0.045	0.064	0.089	0.078	0.054
Nb/Zr	0.03	0.02	0.02	0.02	0.02	0.02	0.04	0.02	0.02
Y/Zr	0.23	0.28	0.28	0.31	0.36	0.32	0.44	0.27	0.34
[La/Sm]cn	0.93	1.47	1.22	1.09	0.87	1.16	1.20	1.26	0.94
[Sm/Lu]cn	1.64	1.50	1.35	1.34	1.25	1.38	1.85	1.44	1.29

N.B.

TK = Tha Tako and KP = Krok Phra. Rhy = rhyodacite/dacite, And = andesite/basalt, and Dio = diorite/gabbro.

Table 5.8 *(Continued)*

Sample number	NKT-092	NKT-111	TK-26	TK-27	TK-37	NKT-031	NKT-051	NKT-101	NKT-112
Rock type	Dio	Dio	And	And	And	And	And	And	And
Area	KP	KP	TK	TK	TK	KP	KP	KP	KP
Sc	22.9	38.4	29.8	40.0	32.9	36.9	36.1	32.6	37.8
Ti	5562	6341	4482	8666	6270	7037	6372	6609	6088
V	170	280	246	269	396	272	252	265	274
Cr	43.8	64.5	24.0	200	13.4	37.2	35.2	88.9	59.7
Mn	1033	1252	1449	1438	1156	1389	1307	1248	1272
Ni	21.8	24.7	32.7	149	9.84	19.2	26.7	39.1	25.7
Cu	38.9	97.7	121	72.4	180	60.0	101	54.4	102
Zn	66.2	77.4	111	170	83.7	86.2	86.3	83.0	74.6
Ga	18.0	16.7	18.8	18.7	18.6	17.8	16.6	17.8	17.6
Ge	1.37	1.26	1.18	1.80	1.90	1.47	1.28	1.24	1.29
Rb	0.78	0.75	7.68	6.17	29.3	1.87	0.84	3.27	1.59
Sr	478	491	445	418	421	431	262	359	460
Y	20.3	21.9	14.5	23.1	19.8	26.7	22.9	26.6	21.7
Zr	79.4	70.6	33.4	94.9	80.0	90.2	67.7	87.4	69.1
Nb	1.59	1.46	0.71	2.18	1.65	1.91	1.24	1.49	1.39
Cs	0.08	0.05	0.38	0.41	2.78	0.11	0.02	0.12	0.07
Ba	56.3	125	66.1	42.6	128	80.9	41.2	67.4	155
La	6.55	5.37	3.77	5.24	7.80	7.32	4.24	6.32	5.39
Ce	15.5	13.2	8.82	13.9	18.3	17.5	11.4	14.4	13.5
Pr	2.31	2.16	1.40	2.32	2.75	2.78	1.94	2.51	2.15
Nd	11.1	10.3	7.10	11.4	12.7	13.5	9.76	12.4	10.4
Sm	2.85	2.80	1.93	3.30	3.19	3.60	2.87	3.48	2.81
Eu	1.07	1.05	0.76	1.25	1.03	1.23	1.05	1.24	1.04
Gd	3.31	3.38	2.37	4.04	3.49	4.33	3.69	4.30	3.47
Tb	0.57	0.62	0.41	0.69	0.58	0.75	0.67	0.77	0.61
Dy	3.48	3.78	2.47	4.16	3.56	4.68	4.05	4.62	3.73
Ho	0.77	0.87	0.55	0.94	0.77	1.07	0.94	1.09	0.83
Er	2.10	2.34	1.54	2.51	2.17	2.96	2.59	2.99	2.31
Tm	0.30	0.35	0.23	0.36	0.31	0.43	0.38	0.43	0.33
Yb	1.98	2.28	1.46	2.27	2.07	2.88	2.51	2.88	2.21
Lu	0.30	0.36	0.23	0.34	0.31	0.43	0.37	0.44	0.34
Hf	2.18	2.01	1.05	2.47	2.28	2.61	1.92	2.49	1.82
Ta	0.17	0.13	0.19	0.26	0.21	0.19	0.13	0.16	0.12
Pb	4.22	4.36	8.82	20.3	6.54	3.33	1.08	2.85	3.16
Th	0.75	0.43	0.21	0.44	1.70	0.68	0.29	0.52	0.41
U	0.30	0.16	0.11	0.17	0.64	0.26	0.13	0.20	0.15
Selected element ratios									
Zr/TiO_2	0.009	0.008	0.005	0.008	0.008	0.008	0.007	0.009	0.007
Nb/Y	0.078	0.067	0.049	0.094	0.083	0.071	0.054	0.056	0.064
Nb/Zr	0.02	0.02	0.02	0.02	0.02	0.02	0.02	0.02	0.02
Y/Zr	0.26	0.31	0.43	0.24	0.25	0.30	0.34	0.30	0.31
[La/Sm]cn	1.40	1.17	1.19	0.97	1.49	1.24	0.90	1.11	1.17
[Sm/Lu]cn	1.59	1.31	1.43	1.63	1.72	1.40	1.31	1.32	1.37

N.B.

TK = Tha Tako and KP = Krok Phra. Rhy = rhyodacite/dacite, And = andesite/basalt, and Dio = diorite/gabbro.

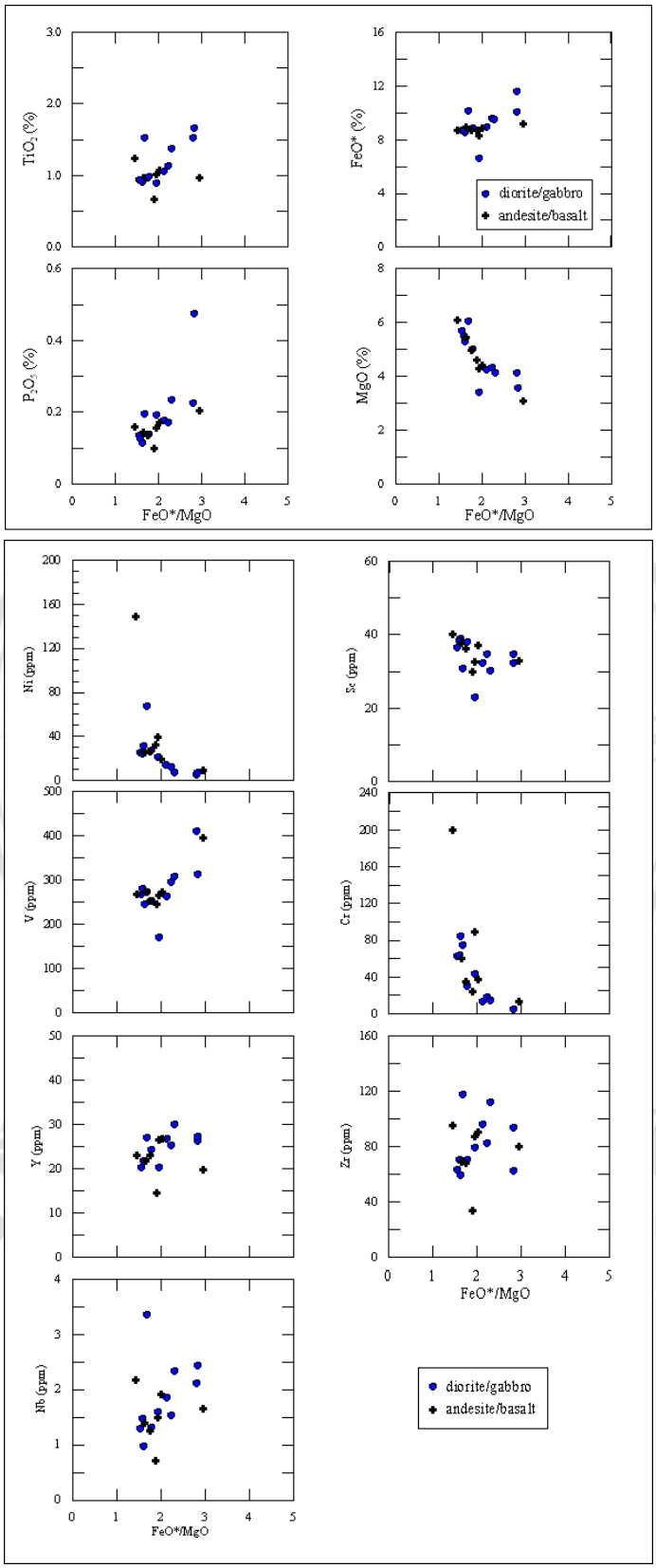

Figure 5.16 FeO*/MgO variation diagrams for immobile major and trace elements of the studied least-altered Group IV rocks.

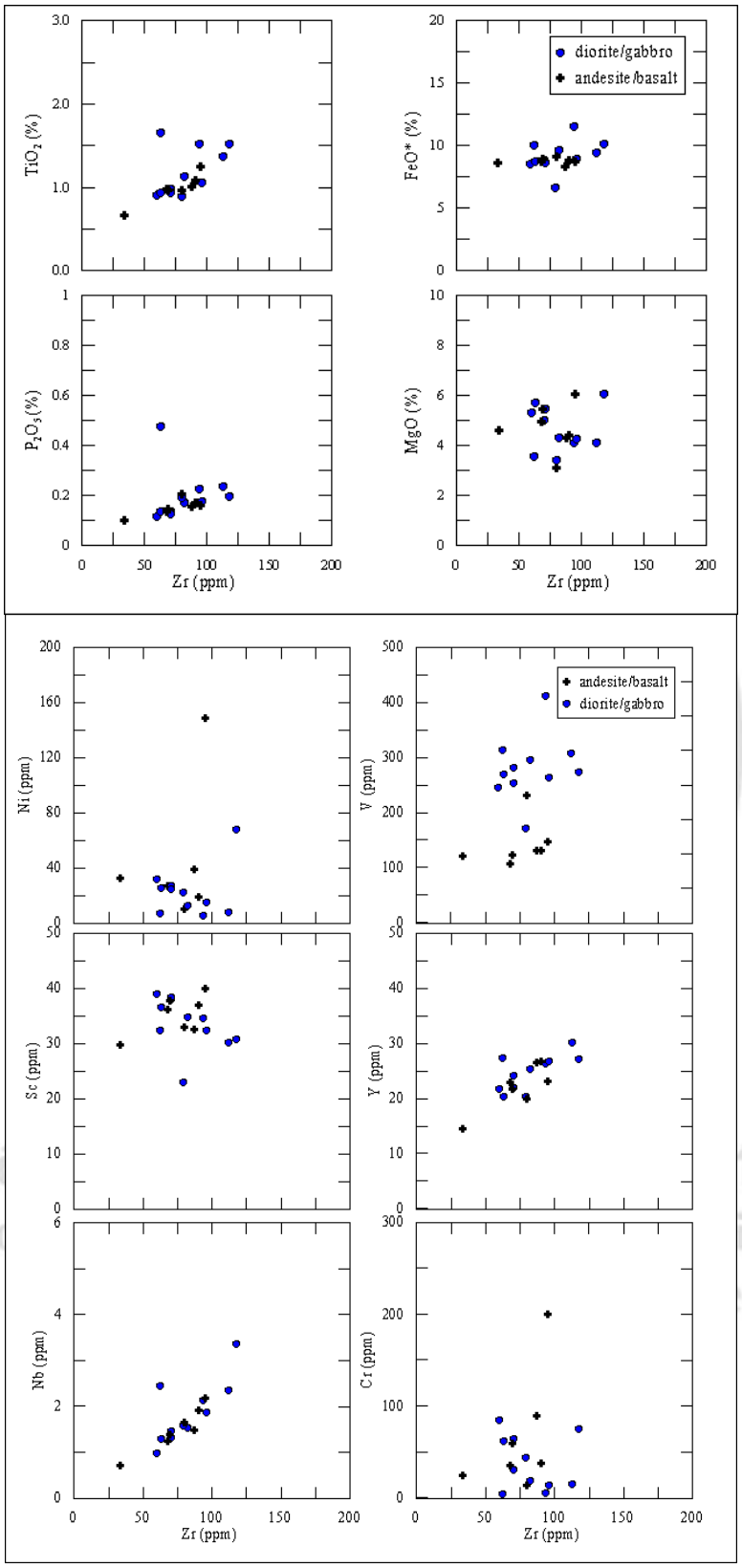

Figure 5.17 Zr variation diagrams for immobile major and trace elements of the studied least-altered Group IV mafic volcanic/hypabassal rocks.

The relationships between incompatible-element pairs for the studied mafic volcanic/hypabassal rock samples, such as Nb-Zr and Y-Zr (Figure 5.17), are linear, with Nb/Zr = 0.022 ± 0.005 and Y/Zr = 0.309 ± 0.058. These signify that all the rocks are essentially co-magmatic. They might have been formed by different degrees of partial melting of a common source rock or by different degrees of crystal fractionation of the same parental magma. The former is unlikely as the patterns for the incompatible-element pairs do not trace back to zero.

The studied subalkalic andesite/basalt suite have chondrite-normalized values for La and Lu in ranges of 11.5 - 28.3 and 7.03 - 15.6, respectively. Their REE patterns (Figure 5.18) are typical of tholeiitic rocks, i.e. LREE and HREE relatively flat, with (La/Sm)cn and (Sm/Lu)cn ranging from 0.87 to 1.49 and 1.25 to 1.84, respectively. In terms of N-MORB normalized multi-element patterns (Figure 5.19), the rocks generally show flat patterns, with negative niobium anomalies. These indicate that the subalkalic Group IV rocks have been crystallized from MORB-like magma that contains a crustal signature. The tholeiitic nature is well supported by their positions on a binary diagram Nb/Y-Ti/Y and ternary diagrams Ti-Zr-Y, Hf-Th-Ta and La-Nb-Y, although the applied diagrams were designed for basalts (see section 5.3).

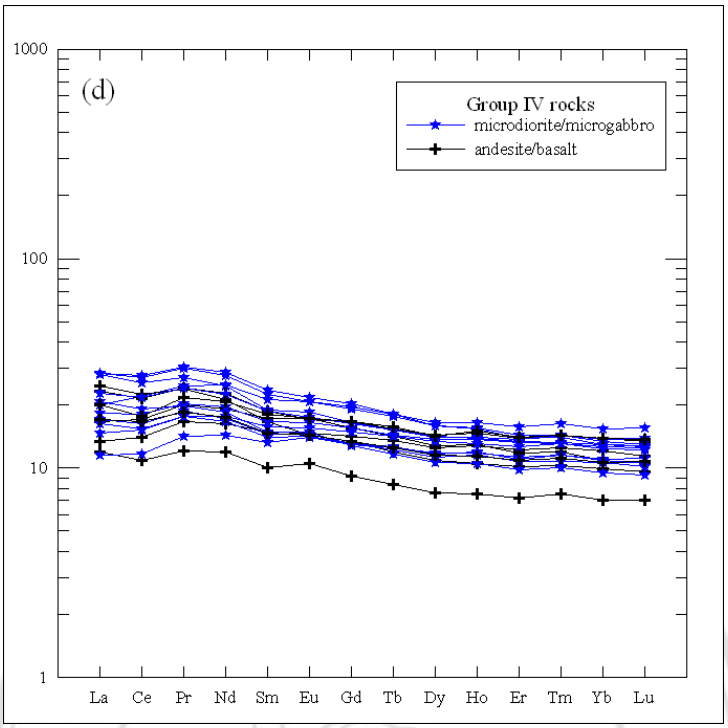

Figure 5.18 Chondrite-normalized REE patterns for the least-altered Group IV rocks presented in this study. The normalizing values used are those of Taylor and Gorton (1977).

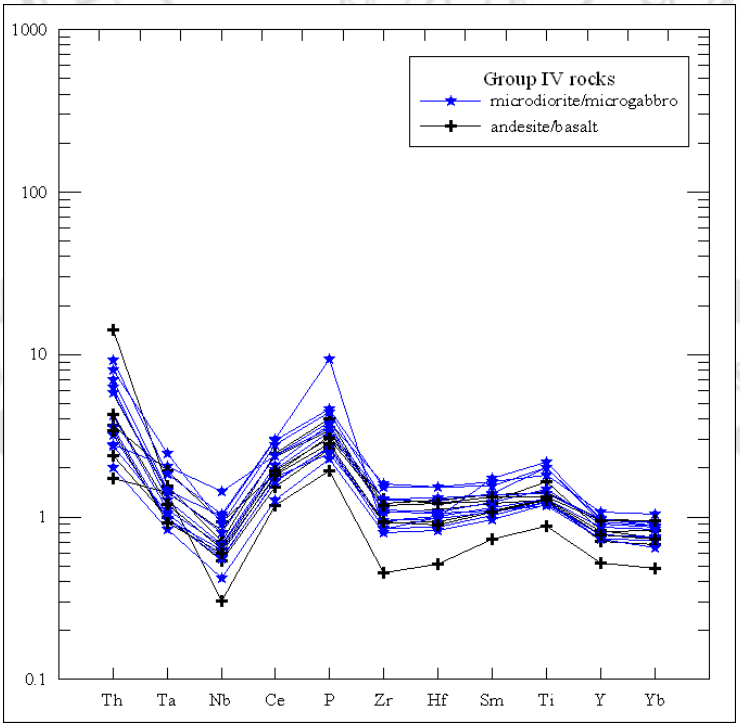

Figure 5.19 N - MORB - normalized patterns for the studied least-altered Group IV rocks. Normalizing values used are those of Sun and McDonough (1989).

5.2.5 Group V rocks

Group V rocks are composed of two samples (KK-02 and KK-20) that were collected from the Tha Tako area, Nakhon Sawan Province. They are nomenclatured as rhyodacite/dacite by the Zr/TiO_2-Nb/Y diagram of Winchester and Floyd (1977) and their textures.

Group V rocks range in Zr/TiO_2 and Nb/Y from 0.038 to 0.039 and 0.20 to 0.21 respectively. They are classified as subalkalic rhyodacite/dacite on the Zr/TiO_2-Nb/Y diagram.

The studied rhyodacite/dacite have chondrite-normalized values for La and Lu in ranges of 80.5 - 188.0 and 9.34 - 12.6, respectively. Their REE patterns (Figure 5.20) are typical of shoshonitic rocks, i.e. LREE (La-Dy) enrichment and relatively flat HREE (Dy-Lu), with (La/Dy)cn and (Dy/Lu)cn ranging from 5.00 to 6.72 and 1.72 to 2.22, respectively. In terms of N-MORB normalized multi-element patterns (Figure 5.21), the rocks generally show flat patterns with negative Nb and Ta anomalies. This suggests that the subalkalic rhyodacite/dacite have characteristics of subduction-related magma.

Table 5.9 Whole-rock XRF major-element analyses of the studied least-altered Group V rocks recalculated to 100 wt% volatile-free, including loss on ignition and original analytical totals.

Sample number	KK-02	KK-20
Rock type	Rhy	Rhy
Area	TK	TK
SiO_2	75.33	73.52
TiO_2	0.31	0.43
Al_2O_3	13.44	16.05
FeO*	2.10	1.84
MnO	0.01	0.04
MgO	0.63	0.20
CaO	2.17	0.57
Na_2O	3.85	7.16
K_2O	2.04	0.13
P_2O_5	0.10	0.08
LOI	3.28	0.85
Original Sum	100.28	99.98
FeO*/MgO	3.33	9.32

N.B.

FeO* = total iron as FeO and LOI = loss on ignition. TK = Tha Tako, and Rhy = rhyodacite/dacite.

.

Table 5.10 Low-abundance trace elements and REE composition (in ppm) for the studied least-altered Group V rocks by ICP-MS analysis.

Sample number	KK-02	KK-20
Rock type	Rhy	Rhy
Area	TK	TK
Sc	8.87	10.4
Ti	2051	2979
V	39.2	19.9
Cr	4.45	4.28
Mn	477	234
Ni	1.24	0.51
Cu	3.26	130
Zn	32.6	57.1
Ga	12.4	7.19
Ge	0.82	1.04
Rb	44.8	2.94
Sr	98.0	213
Y	19.4	28.4
Zr	123	164
Nb	4.12	5.82
Cs	0.47	0.17
Ba	513	120
La	25.4	59.2
Ce	46.4	102
Pr	5.79	11.8
Nd	21.8	44.8
Sm	4.09	9.29
Eu	1.21	2.68
Gd	3.47	7.24
Tb	0.53	1.13
Dy	3.09	5.37
Ho	0.69	1.07
Er	1.84	2.72
Tm	0.28	0.40
Yb	1.92	2.71
Lu	0.30	0.40
Hf	3.47	4.73
Ta	0.41	0.61
Pb	1.41	3.39
Th	6.61	8.46
U	1.72	2.20
Selected element ratios		
Zr/TiO_2	0.039	0.038
Nb/Y	0.213	0.205
Nb/Zr	0.03	0.04
Y/Zr	0.16	0.17
[La/Sm]cn	3.78	3.89
[Sm/Lu]cn	2.28	3.84

N.B.

TK = Tha Tako, and Rhy = rhyodacite/dacite.

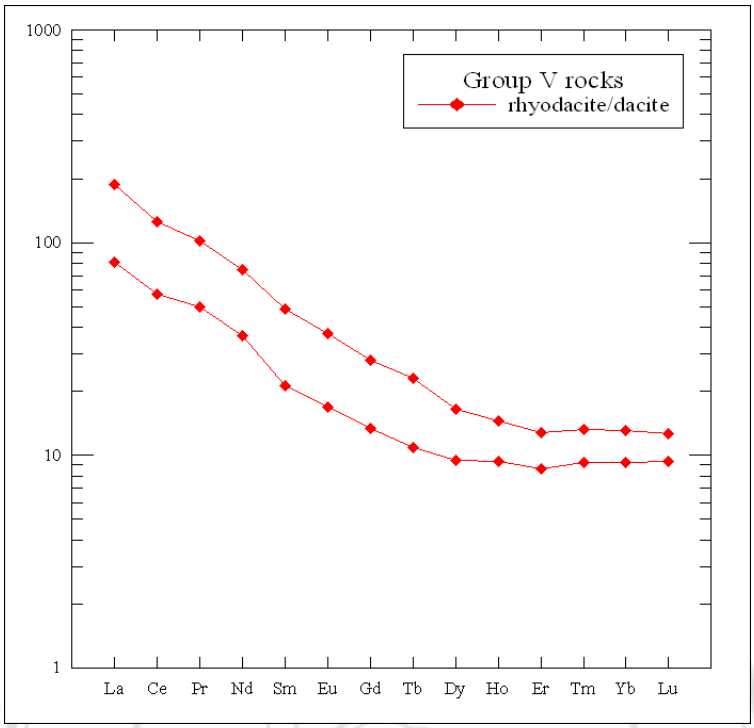

Figure 5.20 Chondrite-normalized REE patterns for the least-altered Group V rocks presented in this study. The normalizing values used are those of Taylor and Gorton (1977).

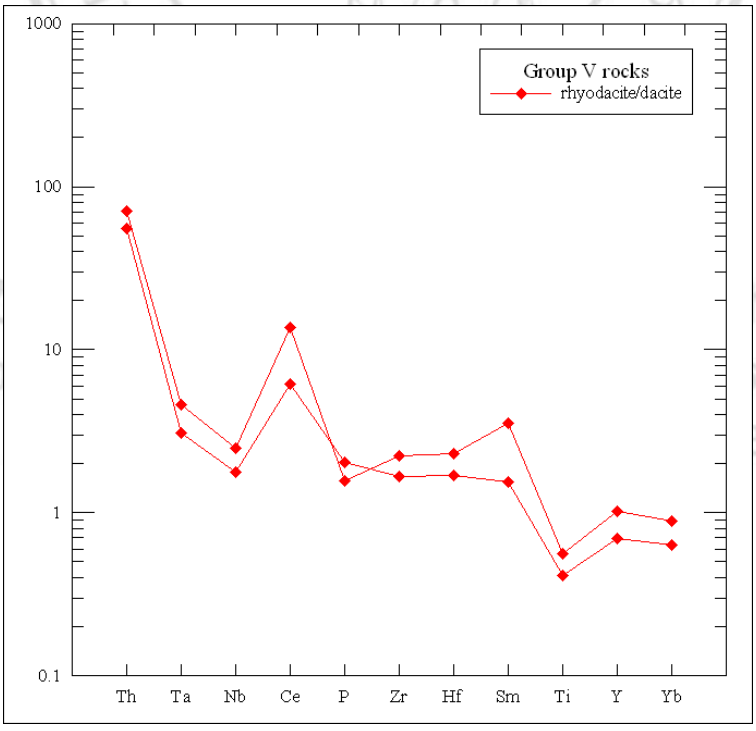

Figure 5.21 N - MORB - normalized patterns for the studied least-altered Group V rocks. Normalizing values used are those of Sun and McDonough (1989).

5.3 Tectonic Setting of Eruption

The relationships between incompatible-element pairs for the studied least-altered felsic to mafic volcanic/hypabassal rocks, such as Nb-Zr and Y-Zr are positively linear, with Nb/Zr = 0.03 ± 0.01 and Y/Zr = 0.23 ± 0.08 (Figure 5.22). These suggest that all the rocks are co-genetic. They might have been formed by different degrees of partial melting of a common source rock or crystal fractionation of the same parental magma. The former is unlikely as the patterns for the incompatible-element pairs do not trace back to zero.

Up to present, many tectonic discrimination diagrams for either mafic or felsic volcanic rocks have been constructed. However, several studies (Holm, 1982; Prestvik, 1982; Duncan, 1987; and Myers and Breitkopf, 1989) have demonstrated that these diagrams may often fail to unequivocally classify tectonic setting of formation of altered lavas. For example, Duncan (1987) studied the Mesozoic basalt of Karoo igneous province, one of the world's classic continental flood basalt. However, it appears that the southern Karoo basalt was erupted in a subduction-related environment, whereas the northern Karoo basalt erupted in a within-plate environment, when tectonic discrimination diagrams were applied. In this study, the felsic to mafic volcanic/hypabyssal rocks have been plotted in many relevant discrimination diagrams and the results are discussed below.

The studied Group I mafic volcanic/hypabyssal rocks appear to be plate-margin basalt, erupted along an active continental margin, an oceanic island arc and a mid-oceanic ridge, on Zr/Y against Ti/Y (Figure 5.23) and Zr/Y against Zr (Figure 5.24) diagrams. These rocks are most likely to have generated in volcanic arc environments on the plots of Ti-Zr (Figure 5.25), Ti/Y-Nb/Y (Figure 5.26), Ti-V (Figure 5.27), Cr-Y (Figure 5.28), Ti-Zr-Y (Figure 5.29), Nb-Zr-Y (Figure 5.30), Hf-Th-Ta (Figure 5.31) and Y-La-Nb (Figure 5.32). In addition, the studied Group I felsic volcanic rocks appear to be volcanic-arc granite or syn-collision granite on Nb-Y (Figure 5.33) and volcanic-arc granite on Rb-(Y+Nb) (Figure 5.34) diagrams.

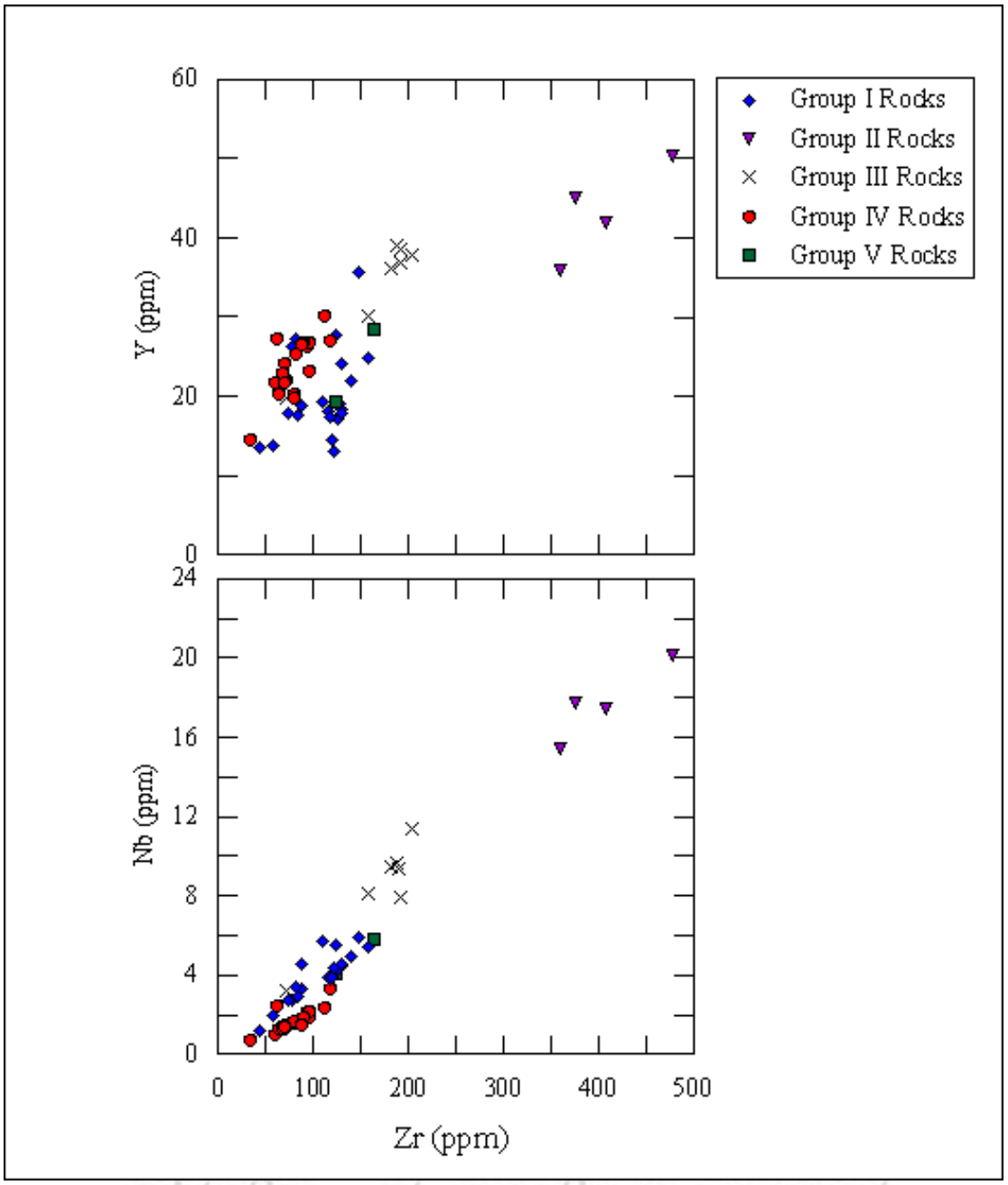

Figure 5.22 Plots of Y and Nb against Zr for the studied least-altered felsic to mafic volcanic/hypabassal rocks.

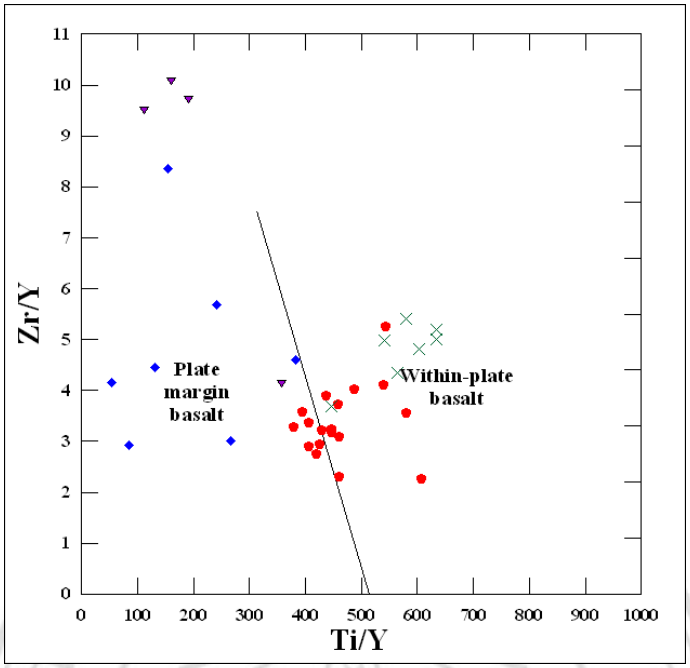

Figure 5.23 Zr/Y-Ti/Y tectonic discrimination diagram (Pearce and Gale, 1977) for the studied least-altered mafic volcanic/hypabassal rocks; Group I (blue diamond), Group II (violet inverted triangle), Group III (green cross) and Group IV (red circle).

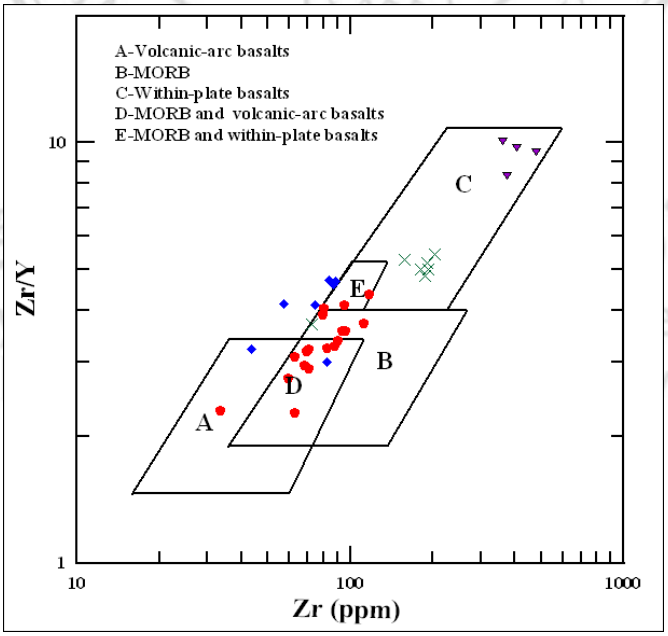

Figure 5.24 Zr/Y –Zr discrimination diagram (Pearce and Norry, 1979) for the studied least-altered felsic to mafic volcanic/hypabassal rocks; Group I (blue diamond), Group II (violet inverted triangle), Group III (green cross) and Group IV (red circle).

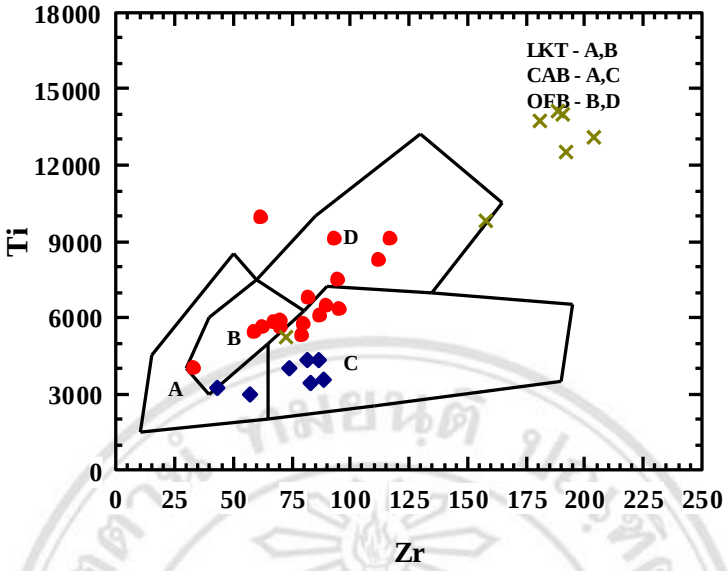

Figure 5.25 Ti-Zr tectonic discrimination diagram (Pearce and Cann, 1973) for the studied least-altered mafic volcanic/hypabassal rocks; Group I (blue diamond), Group II (violet inverted triangle), Group III (green cross) and Group IV (red circle). LKT = low-K theoleiites, CAB = calc-alkalic basalts, and OFB = mid-ocean ridge basalts.

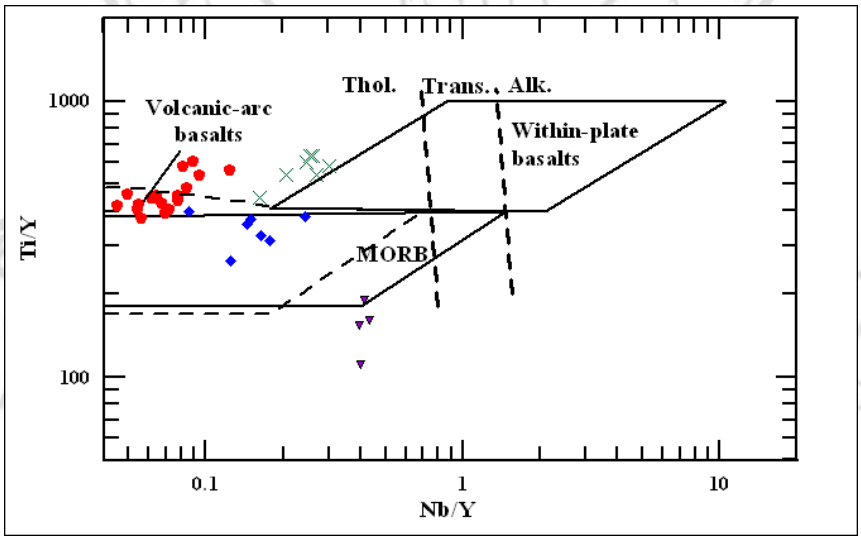

Figure 5.26 Ti/Y – Nb/Y tectonic discrimination diagram (Pearce, 1982) for the studied least-altered mafic volcanic/hypabassal rocks; Group I (blue diamond), Group II (violet inverted triangle), Group III (green cross) and Group IV (red circle). Abbreviations are as follows: MORB = mid-ocean ridge basalts, Thol = tholeiitic, Trans. = transitional tholeiitic, and Alk = alkalic.

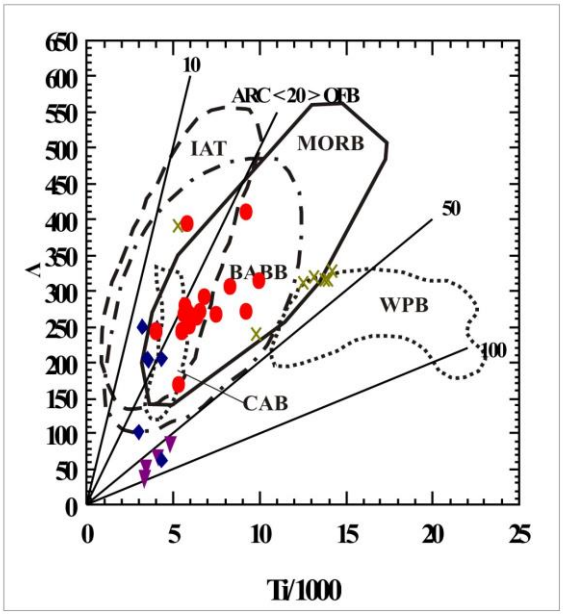

Figure 5.27 Ti-V tectonic discrimination diagram (Shervais, 1982) for the studied least-altered felsic to mafic volcanic/hypabassal rocks; Group I (blue diamond), Group II (violet inverted triangle), Group III (green cross) and Group IV (red circle). The numbers given along the solid straight lines are Ti/V ratios. IAT = island-arc tholeiites, BABB = back-arc basin basalts, WPB = within-plate basalts, and CAB = calc-alkalic basalts.

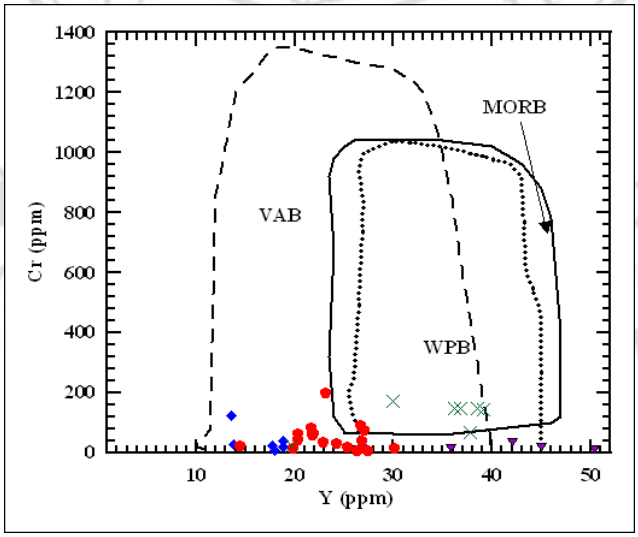

Figure 5.28 Cr-Y tectonic discrimination diagram (Pearce, 1982) for the studied least-altered mafic volcanic/hypabassal rocks; Group I (blue diamond), Group II (violet inverted triangle), Group III (green cross) and Group IV (red circle). VAB = volcanic-arc basalts, MORB = mid-ocean ridge basalts and WPB = within-plate basalts.

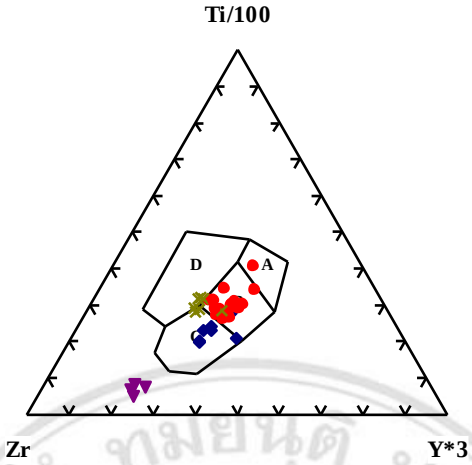

Figure 5.29 Ti- Zr-Y tectonic discrimination diagram (Pearce and Cann, 1973) for the studied least-altered mafic volcanic/hypabassal rocks; Group I (blue diamond), Group II (violet inverted triangle), Group III (green cross) and Group IV (red circle). A = island-arc tholeiites, B = MORB, island-arc tholeiites and calc-alkalic basalts, C = calc-alkalic basalts and D = within-plate basalts.

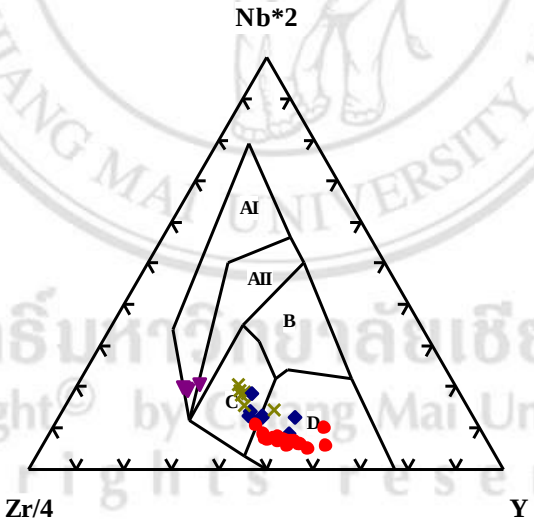

Figure 5.30 Nb-Zr-Y tectonic discrimination diagram (Meschede, 1986) for the studied least-altered mafic volcanic/hypabassal rocks; Group I (blue diamond), Group II (violet inverted triangle), Group III (green cross) and Group IV (red circle). AI = within-plate alkalic basalts, AII = within-plate alkalic basalts and within-plate tholeiites, B = E-type MORB, C = within-plate tholeiites and volcanic-arc basalts, and D = N-type MORB and volcanic arc basalts.

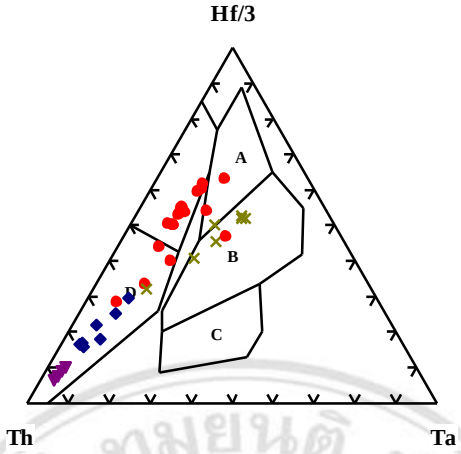

Figure 5.31 Ternary Hf-Th-Ta tectonic discrimination diagram (Wood, 1980) for the studied least-altered mafic volcanic/hypabassal rocks; Group I (blue diamond), Group II (violet inverted triangle), Group III (green cross) and Group IV (red circle). A = N-type MORB, B = E-type MORB and within-plate tholeiites, C = within-plate alkalic basalts, and D = calc-alkalic basalts (Hf/Th<3) and island-arc tholeiites (Hf/Th>3).

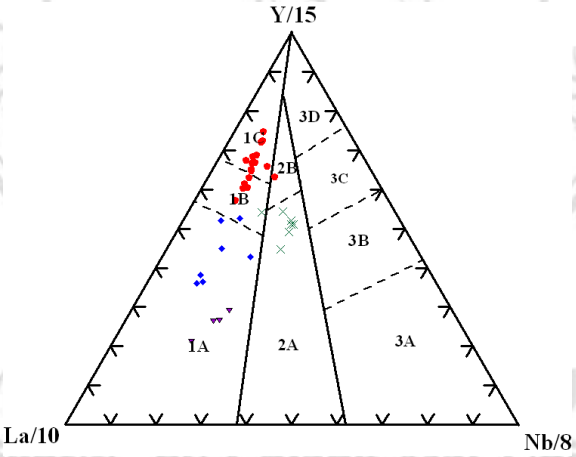

Figure 5.32 Y-La-Nb tectonic discrimination diagram (Cabanis and Le colle, 1989) for the studied least-altered mafic volcanic/hypabassal rocks; Group I (blue diamond), Group II (violet inverted triangle), Group III (green cross) and Group IV (red circle). Field 1 contains volcanic-arc basalts, field 2 continental basalts and field 3 oceanic basalts. The subdivisions of the fields are as follows: 1A = calc-alkalic basalts, 1C = volcanic-arc tholeiites, 1B is an overlap between 1A and 1C, 2A = continental basalts, 2B = back-arc basin basalts, 3A = alkalic basalts from intercontinental rift, 3B and 3C = E-type MORB (3B enriched and 3C weakly enriched), and 3D = N-type MORB.

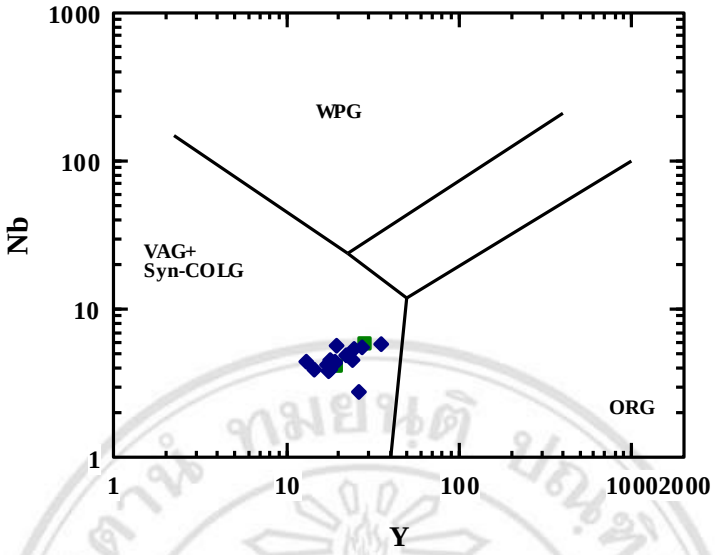

Figure 5.33 Nb-Y tectonic discrimination diagram (Pearce, *el al.*, 1984) for the studied least-altered felsic volcanic/hypabassal rocks; Group I (blue diamond) and Group V (green square). VAG = volcanic arc granites, syn-COLG = syn-collisional granites, WPG = within-plate granites and ORG = ocean-ridge granites.

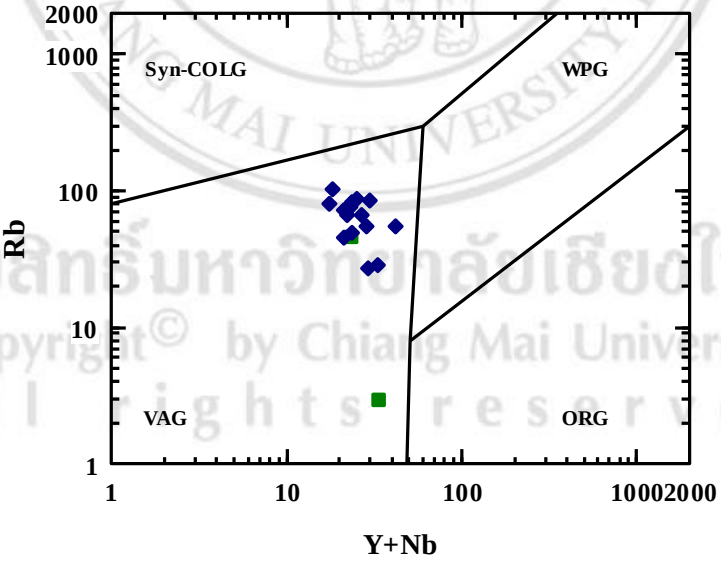

Figure 5.34 Rb-(Y+Nb) tectonic discrimination diagram (Pearce, *el al.*, 1984) for the studied least-altered felsic volcanic/hypabassal rocks; Group I (blue diamond) and Group V (green square). VAG = volcanic arc granites, syn-COLG = syn-collisional granites, WPG = within-plate granites and ORG = ocean-ridge granites.

The studied Group II mafic hypabassal rocks are represent magma or cumulate rock. If the studied Group II mafic hypabassal rocks are represent magma, they are plate-margin basalt on a Zr/Y-Ti/Y plot (Figure 5.23), but within-plate basalt on plots of Zr/Y-Zr (Figure 5.24), Cr-Y (Figure 5.28) and Nb-Zr-Y (Figure 5.30). The plate-margin environment is supported by their positions in the fields of volcanic-arc basalt of Ti-Zr (Figure 5.25), Hf-Th-Ta (Figure 5.31) and La-Y-Nb (Figure 5.32) diagrams. Moreover, the Group II hypabassal rocks lie outside any field of tectonic environments in the plots of Ti/Y–Nb/Y (Figure 5.26), Ti-V (Figure 5.27) and Ti-Zr-Y (Figure 5.29). However, If the studied Group II mafic hypabassal rocks are cumulate rock, they are low Ti ophiolite on a TiO_2 - (FeO*/FeO*+MgO) discrimination diagram (Figure 5.35).

The studied Group III mafic volcanic/hypabassal rocks appear to have many tectonic settings of eruption on different discrimination diagrams. They are within-plate rocks on the plot of Zr/Y-Zr (Figure 5.24), mid-ocean ridge rocks on the plot of Ti-Zr (Figure 5.25) and Nb-Zr-Y (Figure 5.30), volcanic rocks on the plots of Ti-Zr-Y (Figure 5.29), within-plate or mid-ocean ridge rocks on the plots of Ti-V (Figure 5.27) and Hf-Th-Ta (Figure 5.31), and within-plate, mid-ocean ridge and volcanic-arc rocks on the plot of Cr-Y (Figure 5.28). In addition, they are continental basalt on the La-Y-Nb plot (Figure 5.32) and do not fall in any field in the Ti/Y-Nb/Y plot (Figure 5.26).

Of the tectonic discrimination diagrams used, the studied Group IV mafic volcanic/hypabassal rocks appear to be significantly those of mid-ocean ridge (Figures 5.24, 5.25, 5.29 and 5.30) and volcanic-arc (Figures 5.26, 5.28, 5.30, 5.31 and 5.32) environments. They are back-arc basin basalt on the Ti-V plot and have positions straddle on the field boundary between plate-margin and within-plate basalts in Ti/Y and Nb/Y plot (Figure 5.23).

The studied Group V felsic volcanic rocks appear to have formed either in a volcanic-arc environment or in a syn-collision environment as shown in the Nb-Y plot (Figure 5.33). However, they are in the field of volcanic-arc granite on Rb-(Y+Nb) plot (Figure 5.34).

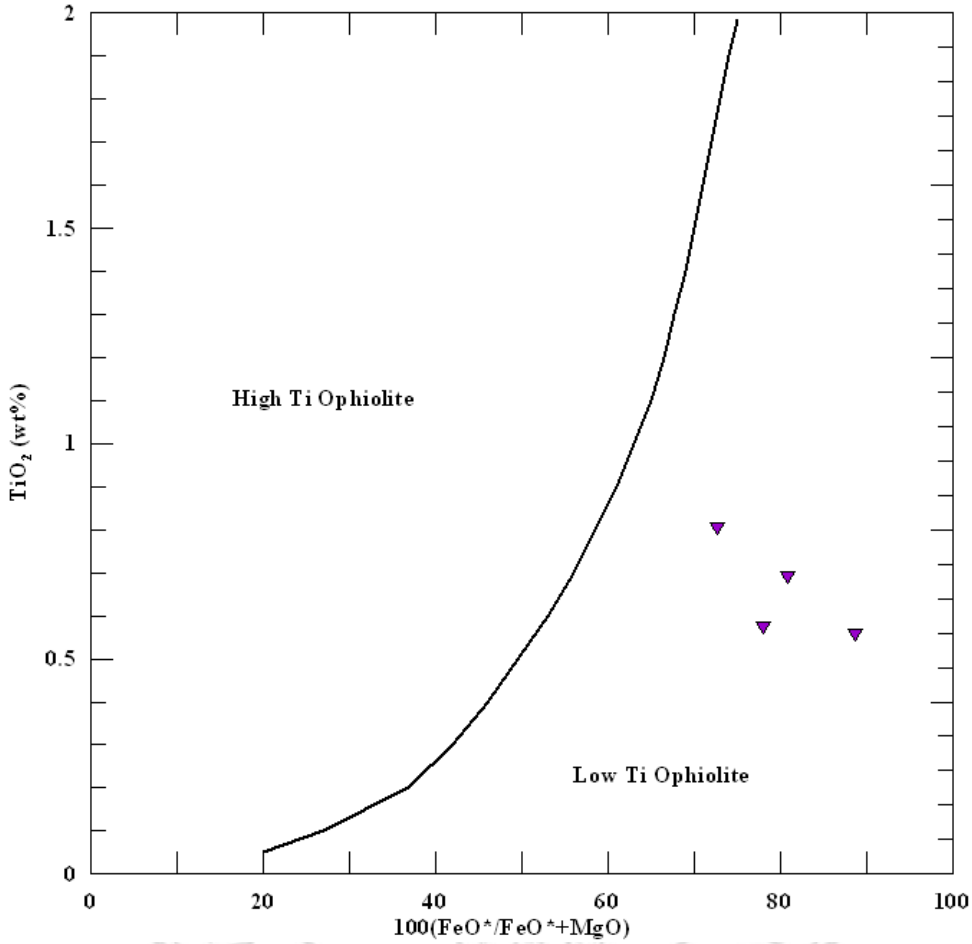

Figure 5.35 TiO_2 – 100(FeO*/FeO*+MgO) discrimination diagram (Serri, 1981) for the studied least-altered mafic hypabassal Group II rocks.

5.4 Modern analogs

Although many tectonic discrimination diagrams have been appeared in literature, a number of workers (e.g. Holm, 1982; Prestvik, 1982; Duncan, 1987; and Myers and Breitkopf, 1989) demonstrated that these diagrams may often fail to clearly classify tectonic setting of formation. In addition, many of these diagrams have no compositional filed for back arc basin basalt. In order to solve the problem, the classical principle of geology "Present is the key to the past" has been applied. In the other words, if the tectonic interpretation is correct, there should be modern analogs (Panjasawatwong, 1991; 1999; Panjasawatwong *et al*., 1995; 1997; 2003; Singharajwarapan *et al*., 2000; Barr *et al.,* 2000). Extensive searches for modern analogs have been made in terms of chondrite and N-MORB normalized multi-element patterns. In doing so, the representatives of the Group I rocks are analogous to the basic rock (sample number S10) from Late Eocene Kuh-e Dom shoshonitic dikes, the Urumieh-Dokhtar magmatic arc, Northeast Ardestan, Central Iran (Sarjoughian *et al.,* 2012) that have developed from remnant melt batches after cessation of active subduction, in post-collision setting (Figures 5.36). The Group II rocks are analogous to the dacite (sample number ER16) from the Quaternary Erciyes volcano, central Anatolia, Turkey (Notsu *et al.*, 1995) that have combined signatures of fractionation crystallization of basaltic magma and crustal assimilation under collision tectonic setting (Figures 5.37). The Group III rocks are analogous to the basaltic andesite (sample number PA-92) from the Quaternary Maca volcano, Patagonian Andes (~45°S, Chile) (D'Orazio *et al.*, 2003) that was erupted in an active continental margin (Figure 5.38). The Group IV rocks are analogous to the basalt (sample number As-5) from the Pliocene Asahiura basalt, Eastern zone, Southwest Hokkaido, northern NE Japan arc (Takanashi *et al.*, 2011) that was erupted in an active continental margin (Figure 5.39). The Group V rocks are analogous to the intermediate rock (sample number S15) from Late Eocene Kuh-e Dom shoshonitic dikes, the Urumieh-Dokhtar magmatic arc, Northeast Ardestan, Central Iran (Sarjoughian *et al.*, 2012) that have developed from remnant melt batches after cessation of active subduction, in post-collision setting (Figure 5.40).

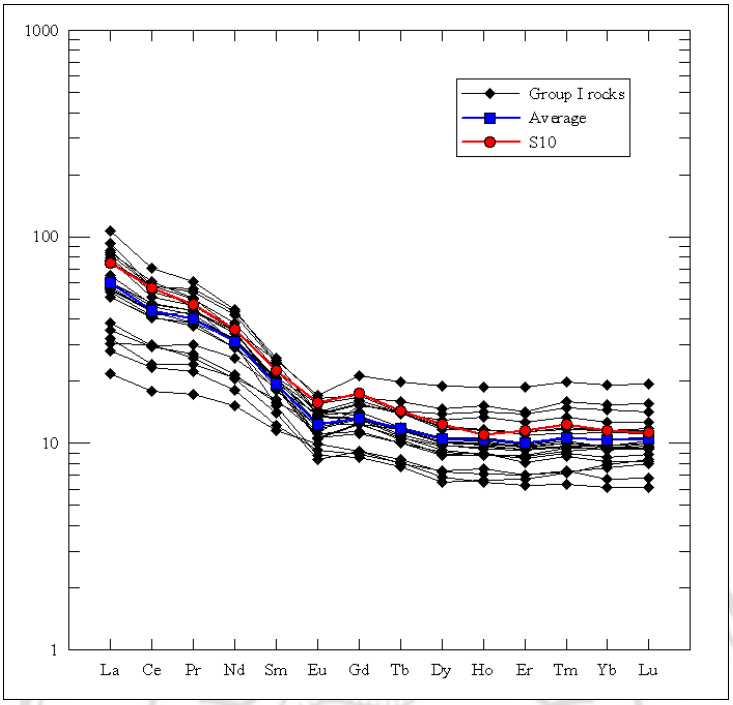

(a)

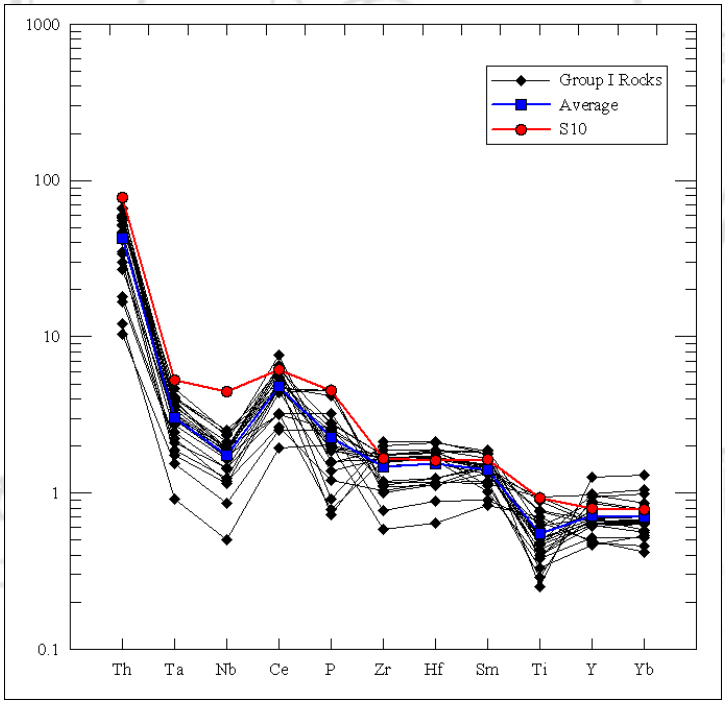

(b)

Figure 5.36 Plots of (a) chondrite-normalized REE and (b) N-MORB normalized muti-element patterns for the representatives of Group I rocks and their modern analog, a basic rock (sample number S10) from Late Eocene Kuh-e Dom shoshonitic dikes, the Urumieh-Dokhtar magmatic arc, Northeast Ardestan, Central Iran (Sarjoughian *et al.*, 2012). Chondrite-normalizing values are those of Taylor and Gorton (1977), where N-MORB normalizing values are those of Sun and Mcdonough (1989).

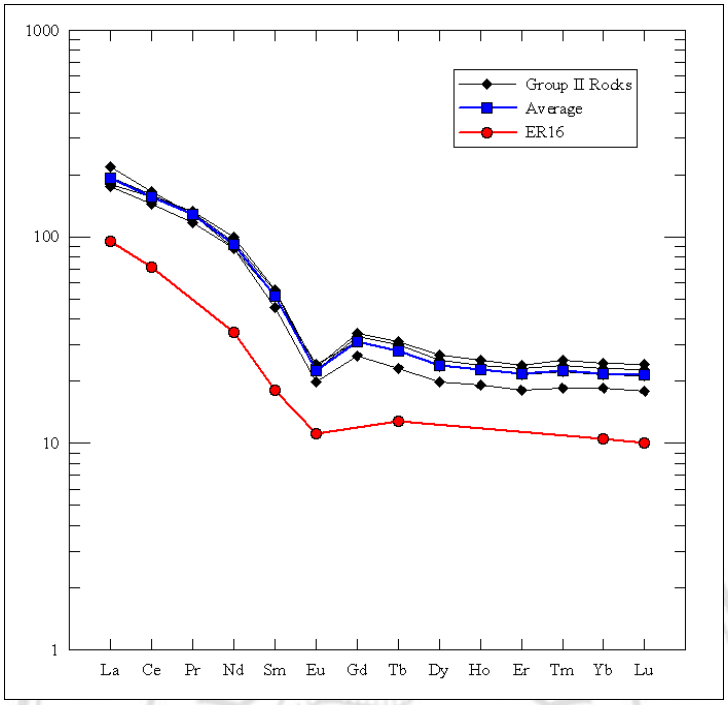

(a)

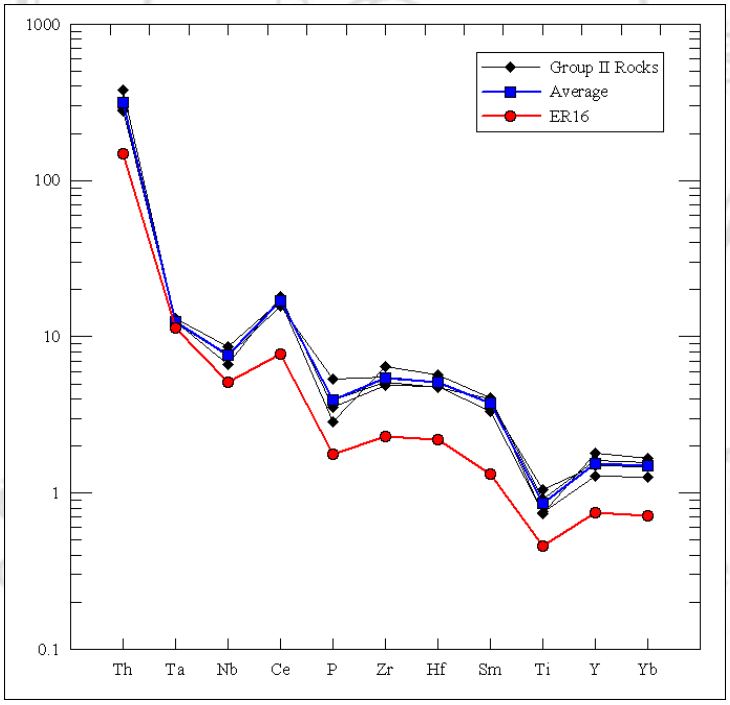

(b)

Figure 5.37 Plots of (a) chondrite-normalized REE and (b) N-MORB normalized muti-element patterns for the representatives of Group II rocks and their modern analog, dacite (sample number ER16) from the Quaternary Erciyes volcano, central Anatolia, Turkey (Notsu *et al.*, 1995). Chondrite-normalizing values are those of Taylor and Gorton (1977), where N-MORB normalizing values are those of Sun and Mcdonough (1989).

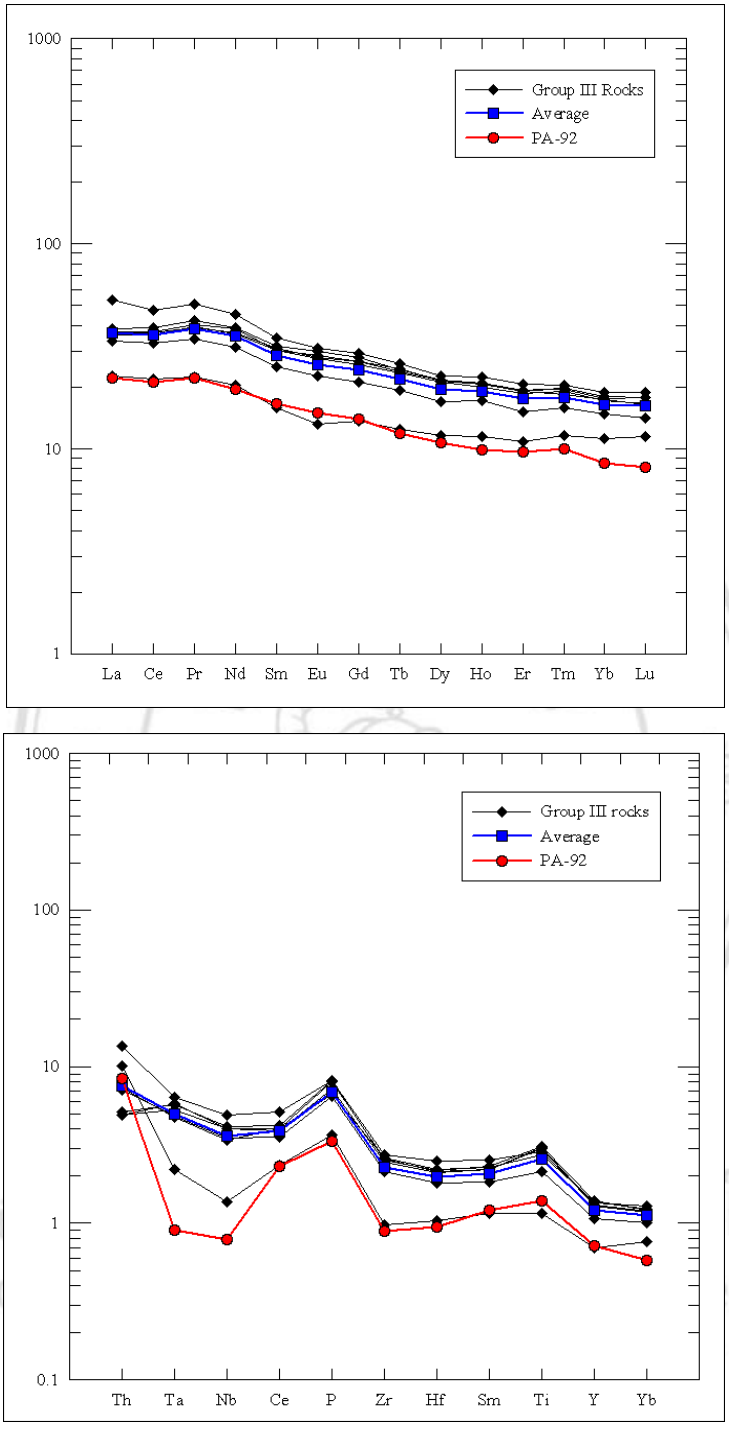

Figure 5.38 Plots of (a) chondrite-normalized REE and (b) N-MORB normalized muti-element patterns for the representatives of Group III rocks and their modern analog, basaltic andesite (sample number PA-92) from the Quaternary Maca volcano, Patagonian Andes (~45°S, Chile) (D'Orazio *et al.*, 2003). Chondrite-normalizing values are those of Taylor and Gorton (1977), where N-MORB normalizing values are those of Sun and Mcdonough (1989).

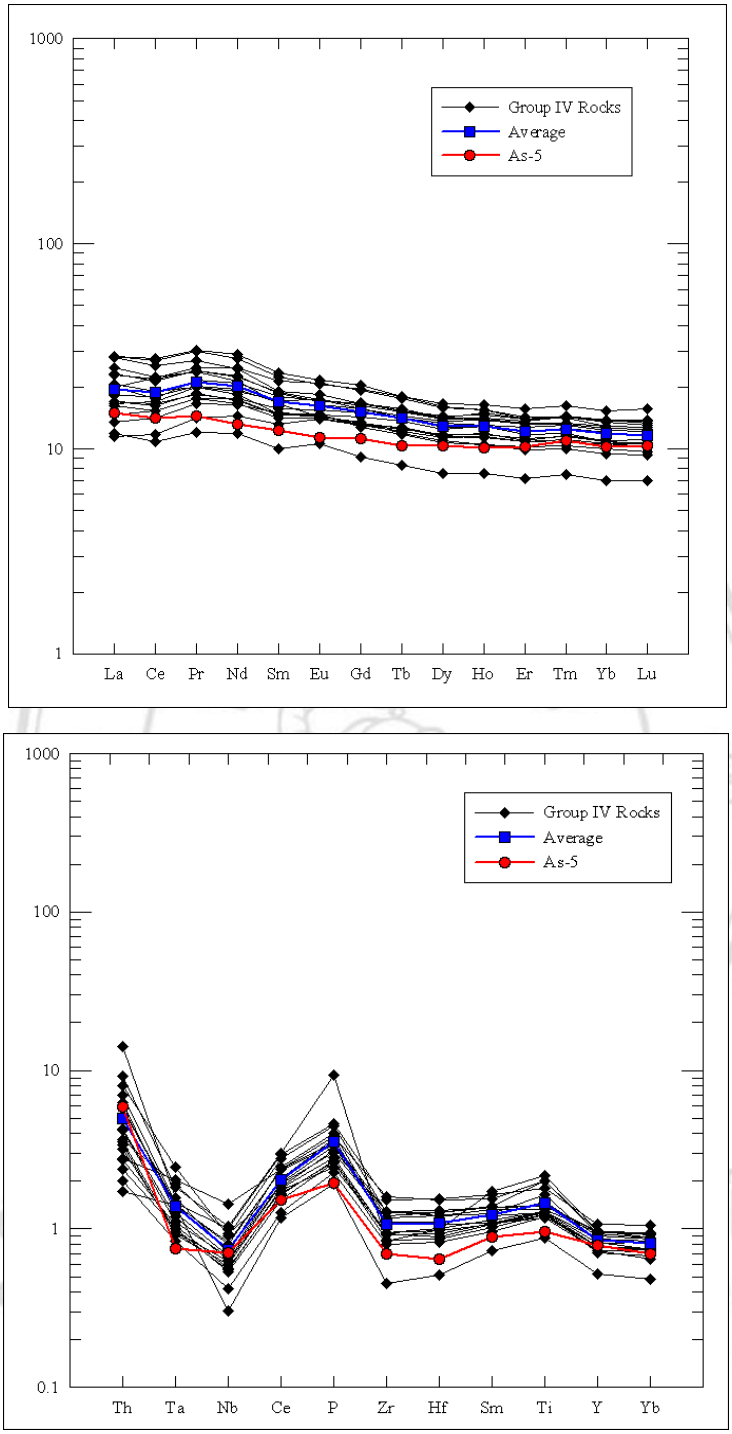

Figure 5.39 Plots of (a) chondrite-normalized REE and (b) N-MORB normalized muti-element patterns for the representatives of Group IV rocks and their modern analog, basalt (sample number As-5) from the Pliocene Asahiura basalt, Eastern zone, Southwest Hokkaido, northern NE Japan arc (Takanashi *et al.*, 2011). Chondrite-normalizing values are those of Taylor and Gorton (1977), where N-MORB normalizing values are those of Sun and Mcdonough (1989).

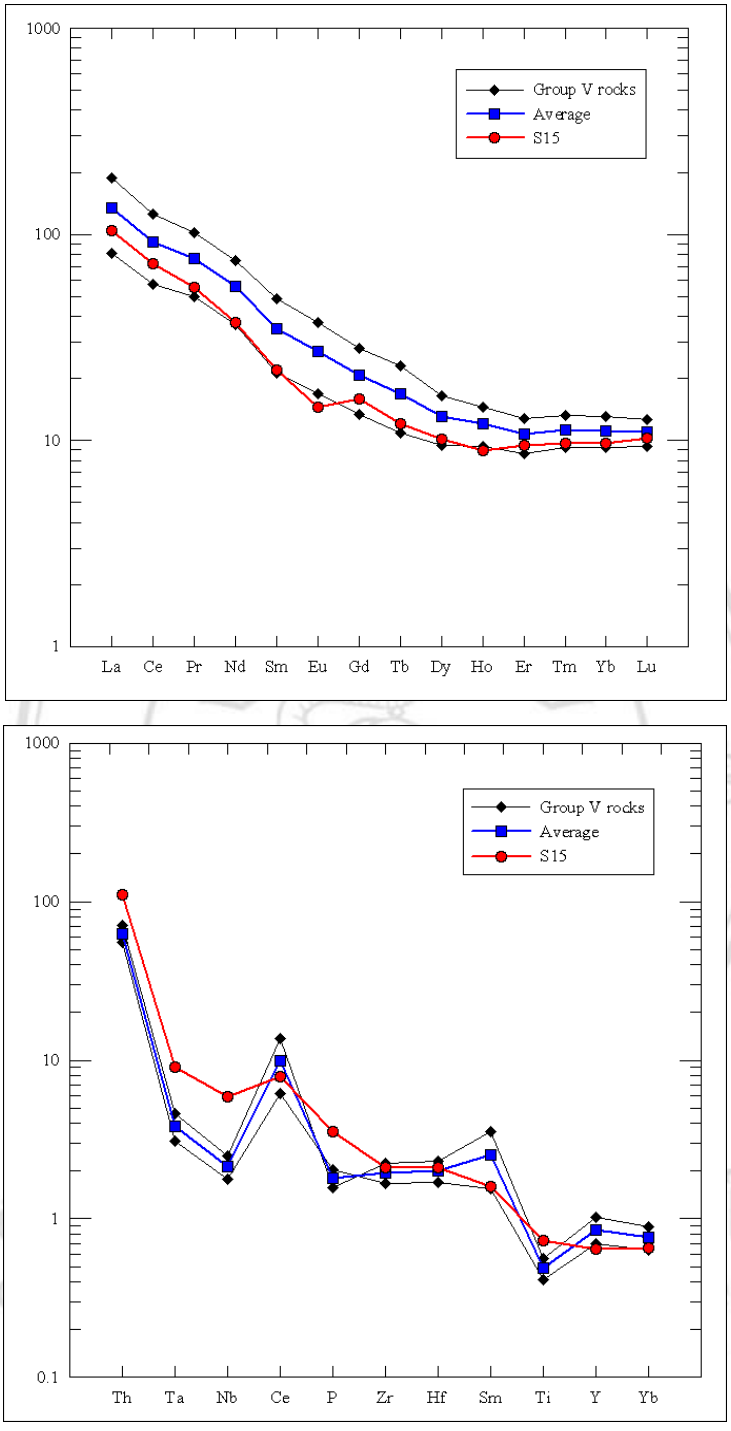

Figure 5.40 Plots of (a) chondrite-normalized REE and (b) N-MORB normalized muti-element patterns for the representatives of Group V rocks and their modern analog, an intermediate rock (sample number S15) from Late Eocene Kuh-e Dom shoshonitic dikes, the Urumieh-Dokhtar magmatic arc, Northeast Ardestan, Central Iran (Sarjoughian *et al.*, 2012). Chondrite-normalizing values are those of Taylor and Gorton (1977), where N-MORB normalizing values are those of Sun and Mcdonough (1989).